BEHAVIOR OF COMPOSITE BRIDGES AT

EARLY AGES AND UNDER THERMAL LOADING

By
ALANNA WEBB

Bachelor of Science in Civil Engineering
Oklahoma State University
Stillwater, OK
2016

Submitted to the Faculty of the
Graduate College of the
Oklahoma State University
in partial fulfillment of
the requirements for
the Degree of
Master of Science
December, 2018

BEHAVIOR OF COMPOSITE BRIDGES AT

EARLY AGES AND UNDER THERMAL LOADING

Thesis Approved:

Dr. Bruce Russell

Thesis Adviser

Dr. M. Tyler Ley

Dr. Robert Emerson

ACKNOWLEDGEMENTS

I would like to acknowledge the Oklahoma Department of Transportation for funding this research work. Thank you to Dr. Bruce Russell for giving me the opportunity to work with him during my Masters and mentoring me through my academic career. I would also like to thank Dr. Tyler Ley and Dr. Robert Emerson for agreeing to serve on my committee. Hema Jayaseelan, Tanner Bridenstein, Justin Smith, and Morgan McBride: it was a pleasure to work with all of you on this research. A very special thanks to my parents, husband, and the rest of my family and friends for all of their support and encouragement throughout my years of study and through the process of researching and writing this thesis. This accomplishment would not have been possible without them.

Name: ALANNA WEBB

Date of Degree: DECEMBER, 2018

Title of Study: BEHAVIOR OF COMPOSITE BRIDGES AT EARLY AGES AND UNDER THERMAL LOADING

Major Field: CIVIL ENGINEERING

Abstract: This paper focuses on deflections and deformations that occur at early ages and under thermal loading in newly rehabilitated bridges comprised of steel girders made composite with concrete deck slabs. A full-scale prototype bridge was constructed at the Bert Cooper Engineering laboratory. The prototype matches the Eagle Chief Creek (Bridge "A") on SH14 in Woods Co. A large array of sensors and instruments were installed to measure strains, deflections, and temperature in both concrete and steel.

Concrete decks cast on steel bridge girders change in volume immediately upon taking initial set. Volume changes are caused by elevated temperature during curing, drying shrinkage, and creep. A large proportion of drying shrinkage occurs at early ages; this has led some to theorize that concrete shrinkage is responsible for poor elevation control of concrete bridge decks. Our research findings indicate that the primary cause for poor ride quality is poor elevation control during construction operations.

Concrete bridge decks are also subject to repeated temperature changes that cause temperature gradients through the depth of the slab producing internal thermal stresses that directly result in bridge deformations. Volumetric changes in concrete lead to upward and downward bridge deflections, differential strains and the resulting internal stresses within the concrete. The cumulative effect of these phenomena can adversely affect the ride quality, cause excessive deflections, decrease durability and reduce the long-term performance of steel girder bridges made composite with concrete decks.

TABLE OF CONTENTS

LIST OF TABLES

LIST OF FIGURES

CHAPTER I

INTRODUCTION

1.1 BACKGROUND

Volume changes in the concrete deck affect the serviceability and durability of the bridge. Knowing the volume changes in the concrete are important in understanding the bridge performance. We need to know the short term and long term material properties, which include: compressive strength, tensile strength, elastic modulus, etc. We also need to know the creep and shrinkage characteristics of the concrete and the reaction of the bridge to temperature and temperature gradients through the slab and the cross section. Many existing bridges in Oklahoma with steel girder superstructures have been rehabilitated by casting new concrete deck slabs atop the existing steel girders. After bridges were rehabilitated, it was found that the ride profiles were uneven and that elevations of the bridge deck were generally lower near the middle regions of the bridge spans. It has been suggested that some of these deflections are caused by drying shrinkage of the concrete.

The majority of concrete shrinkage begins immediately upon the concrete taking initial set, and continues long after concrete has hardened. During hydration, some water is consumed by the hydration process; as hydration continues after initial set, water that is consumed from the pore spaces may cause internal negative pressure that results in

shrinkage. Additionally, shrinkage results as water evaporates from the concrete which can also cause negative pressures in the pore spaces. Shrinkage will not occur until initial set takes place, but the negative pressures in pore spaces caused by evaporation can continue long after the concrete has hardened and curing has been completed. Good predictions of the volume changes during the early ages of a bridge are important for structures where serviceability is highly considered. However, excessive or unexpected shrinkage usually does not result in structural failure.

In addition to the early age behaviors affected by the hydration process, creep, and shrinkage in concrete bridge decks, we must also consider the behavior of bridges under thermal loading. The prototype bridge measurements show the significance of temperature gradients produced by summertime heat loadings. Additional strains and deflections occur when a bridge is subjected to the cyclic thermal loads generated by normal weather conditions.

1.2 SCOPE

In our research, a prototype bridge was constructed from steel girders made composite with a concrete deck slab. The bridge was monitored for short term deflections, temperatures, inclinations, concrete strains, and steel strains to determine the effects of time dependent properties of concrete decks on the deflections of steel girders. Additionally, the bridge was monitored during thermal loading to determine the temperature induced deformations, strains, inclinations, and temperature gradients. This work focuses on the early age behavior of bridges and also includes the effects of temperature loading. Research and test results will provide information on the influence

of early age properties and thermal loads on the serviceability of rehabilitated composite steel girder concrete deck bridges, primarily regarding excessive deflections.

1.3 OBJECTIVES

The objectives of the research are:

- Determine the impact of time dependent volume changes on the serviceability of concrete bridge decks.
- Determine the short-term and near-term properties of concrete and relate those properties to the composite bridge behavior.
- Determine causes for unwanted deformations in composite concrete/steel girder bridges.
- Determine if concrete shrinkage contributes to downward deflections in constructed bridge spans.
- Determine the impact of temperature loadings on the serviceability of concrete bridges.
- Determine the temperature gradient of the prototype and compare to the AASHTO design temperature gradient.

CHAPTER II

LITERATURE REVIEW

2.1 BACKGROUND

A bridge that is structurally deficient has significant deterioration or defects of the bridge deck, superstructure, or substructure. In 2010, 706 bridges in Oklahoma were classified as structurally deficient. The number of structurally deficient bridges in 2017 had been reduced to 185, a 74% reduction between 2010 and 2017 (ODOT 2018). The Oklahoma Department of Transportation (ODOT) is committed to reducing the number of structurally deficient bridges in the state and the current eight-year plan includes improvements on all of the known structurally deficient bridges.

Many of these structurally deficient bridges are being rehabilitated in order to minimize costs while improving the quality and maximizing the life span of the bridges. Some of these bridges were originally built with a concrete deck on steel girders and have been rehabilitated by casting a new concrete deck slab on top of the existing steel girders. In 2012, a bridge in Woods Co. Oklahoma was found to possess poor ride quality due to excessive deflections. In addition to this bridge, one in Payne Co. and one near Eufaula were identified.

2.2 COMPOSITE ACTION IN CONCRETE/STEEL GIRDER BRIDGES

Composite action in structures can be defined as the interaction of different structural elements in which the materials act as a single unit under superimposed loads. Bridges consisting of a cast-in-place reinforced concrete slab on a steel beam are one of the most common composite structures. Steel studs are the most common method for providing composite action between the concrete deck and steel girders. In the design of composite steel and concrete structures, the engineer has to understand the mechanisms of composite behavior between the components.

Oehlers and Bradford (2013) state that there are several reasons for combining steel and concrete elements to form composite members. Non-composite action will occur when there is little or no connection between the elements. The steel and concrete will act independently as two separate beams with a neutral axis at the center of gravity for each element (Olsson, Hällmark et al. 2017). Figure 2.1 illustrates the slipping between the steel and concrete in a non-composite structure.

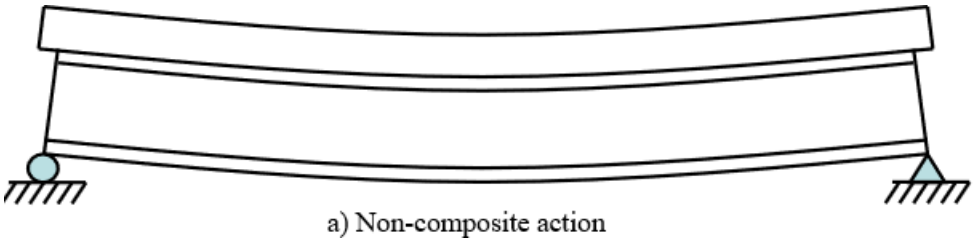

Figure 2.1: Non-composite action where the slip is visible at ends (Kwon, Hungerford et al. 2007).

When the steel and concrete are bonded together in structures resisting gravity loads, the steel is often subject to tension whereas the concrete resists compression. This can

increase the flexural strength and stiffness of the beam leading to reductions in span to depth ratios and overall cost savings.

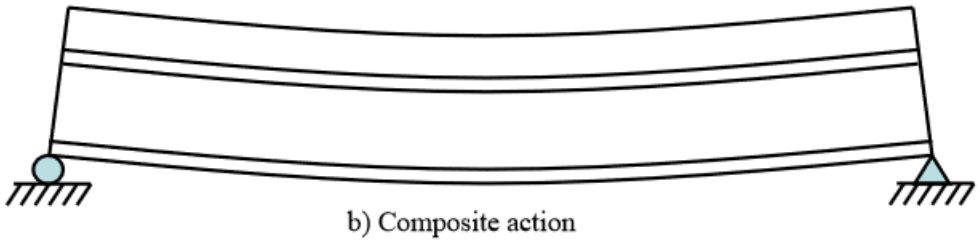

Figure 2.2: Full composite action with no slip between the two elements (Kwon, Hungerford et al. 2007)

Full composite action is achieved when there is a total interaction between the elements. This interaction is a result of the shear connectors or other bond elements preventing slip between the interface of the steel and concrete. For full composite action to occur, the shear studs must be strong enough and stiff enough to withstand movement of the steel girders relative to the concrete (Olsson, Hällmark et al. 2017). The behavior of composite action is illustrated in Figure 2.2.

2.3 INFLUENCE OF HYDRATION ON CONCRETE DECKS

Concrete is formed from a chemical reaction, called hydration, between water and cement. The heat that is released by hydration of one mole of ions at a constant pressure is defined as the heat of hydration. The process of hydration can be broken into six stages as depicted in Figure 2.3.

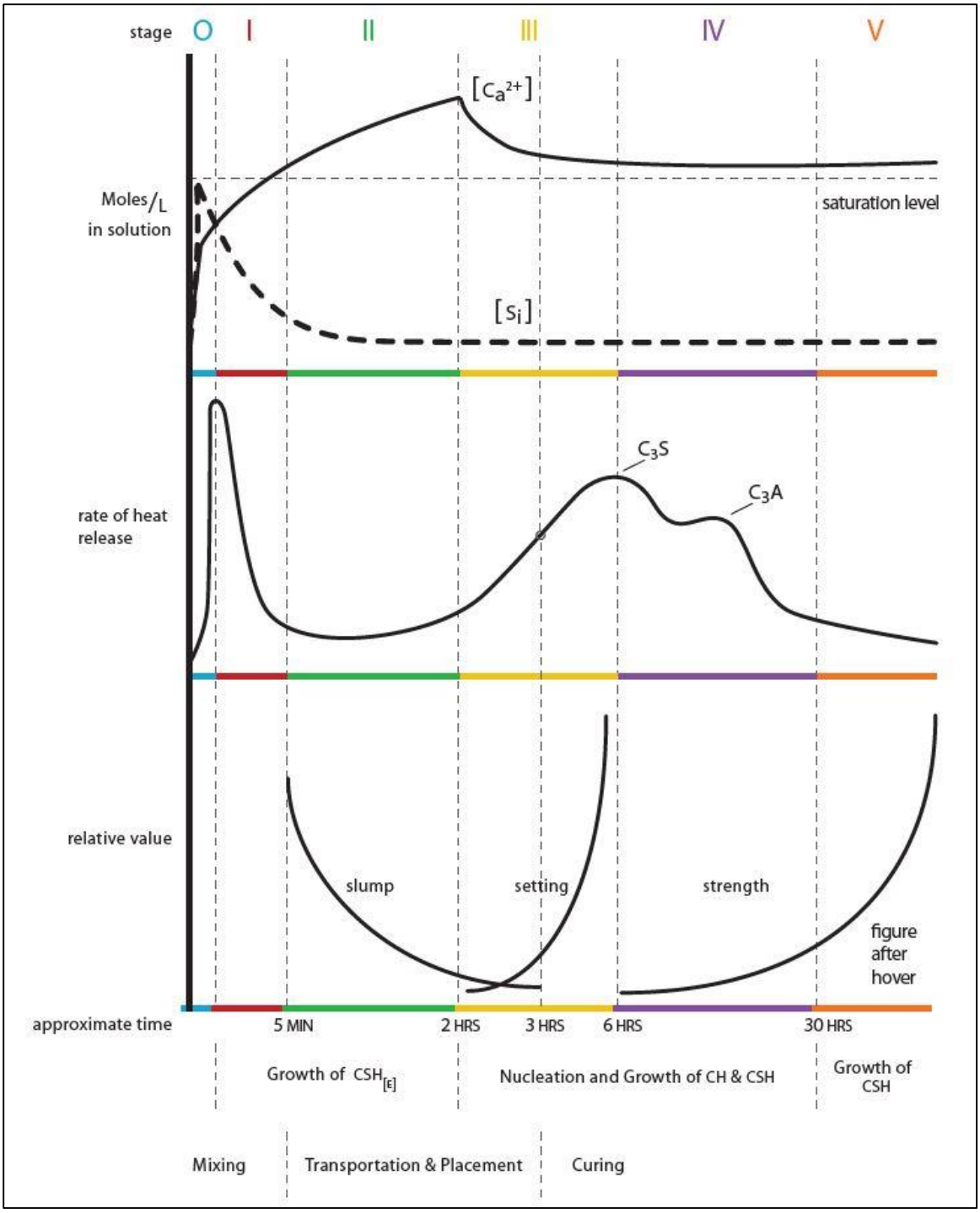

Figure 2.3 – Portland Cement Hydration (Ley 2012)

Stage 0 and 1 comprise the mixing period of the hydration process. During Stage 0 of the hydration process, cement is added to water. Hydrolysis occurs as CA++ ions are

dissolved in solution, and early age calcium silicate hydrate (C-S-H) and ettringite (A_{ft}) are formed. Many chemical reactions occur during these stages. In Stage 1, the surface of a cement particle "changes" as ettringite forms a diffusion barrier and it becomes difficult for water to access cement grains.

During Stages 2 and 3, the concrete is transported and placed. Stage 2 is known as the induction period. There is very little heat given off during this stage as it is still difficult for water to reach the cement grain. Stage 3 is the acceleration period. In this stage, calcium concentration reaches a supersaturated level. Calcium hydroxide (CH) begins to form within the solution and the cement surface changes. Additionally, C-S-H forms rapidly and A_{ft} nucleates on the surface causing initial set. After 6 hrs., concrete reaches a deceleration period or Stage 4. Hydration slows as C-S-H forms on the surface of the cement grain and the reaction becomes diffusion controlled. Beyond 30 hrs., hydration proceeds at a slow rate as long as water is available. Hydration will cease if the water is removed from the system; this is why curing is so important.

Research by Subramaniam, Kunin et al. (2010) investigated the thermal movements and stress in the concrete deck and steel girders due to changes in temperature introduced by the heat of hydration release that occurred during the first few hours after casting the concrete deck. This paper focuses on the correlation between temperature changes and cracking. A single span, simply supported steel girder bridge with composite concrete deck was selected and instrumented. Temperature and strain data for both concrete and steel was recorded before, during, and after placement of the deck. The data was

analyzed to assess thermal movement of the concrete deck and steel girder and their contribution to early age stresses in the concrete deck.

A single span, simply supported field bridge with no skew and a composite concrete deck with steel girders was selected for instrumentation. The bridge was constructed in three stages and Stage 1 of the construction period was instrumented. Stage 1 of the bridge consisted of three girder lines with a span of 106.3 ft c/c of bearing and spaced at 9.6 ft supporting a concrete deck 24.7 ft wide and 9.4 in. thick. A varying haunch depth of 2 in. to 4 in. was provided along the span. Three rows of shear stud connectors at 6.9 in. spacing were provided on the top flange along the span of the steel girders. The steel girders were a built up section consisting of 2 in. x 17.7 in. flanges and 0.5 in. x 47.2 in. web plate sections. In addition, angle sections spaced at 17.7 ft along the span were provided as diaphragms. The steel girders were supported over fixed bearings on one end and expansion bearings on the other support. The concrete deck was placed one day after the placement of reinforcing bars and was moisture cured for 14 days with wet burlap. The concrete mix design conformed to the high-performance mix design of the New York state DOT.

The bridge was instrumented with four vibrating wire strain gages all positioned at the same vertical plane along the cross section of the bridge at the mid span location for the bridge. Two vibrating wires were embedded in the concrete deck, each one attached to the top and bottom reinforcing mat respectively. Each of the other two vibrating wire strain gages were epoxy mounted to the bottom surface of the top flange and top surface of the bottom flange of steel girders. All the strain gages were positioned in the

longitudinal direction along the span of the bridge. The changes in strain and the temperature in both concrete and steel were recorded from 2 hrs. before cast until 7 days after cast.

At about 12 hrs. after slab cast, it was observed that there was gradual increase in the strain readings between the concrete deck and the top of the steel flange. This phenomenon was related to the initial increase in temperature associated with the heat of hydration which was then followed by a decrease in strain that continued up to 48 hrs. after cast. It was also observed that during the first 48 hrs. of curing there was large variation of strain readings between the concrete deck and top of steel flange. Beyond the 48 hrs., at the end of the cooling period, full strain compatibility between the concrete deck and the top flange of the steel girder was observed and the strain readings corresponded well with the ambient temperatures. From the analysis of the data, the paper concludes that at the end of the heat of hydration period the concrete deck gains sufficient stiffness and restrains the movement of the top flange of the girder. Concrete begins to set at the end of the heating period and has lower tensile strength. A large temperature gradient in the steel girder at the end of the heating period induces larger tensile stresses in the concrete which may increase the likelihood for concrete to crack. It was also found that larger differences in temperature between the concrete deck and the top flange of the steel girder at the end of the cooling period can contribute to larger magnitudes of tensile stresses in the concrete deck. The paper proposes that the use of proper design and construction practices that ensured small variations in thermal strain and temperature between the concrete and the steel girder can help minimize the thermal tensile stress induced in concrete deck slabs.

2.4 EFFECTS OF CONCRETE SHRINKAGE ON COMPOSITE STEEL BEAMS

There are two primary types of shrinkage in concrete – drying shrinkage and autogenous shrinkage. Drying shrinkage is the result of water loss in hardened concrete. As the water evaporates from the concrete, the volume of concrete reduces. Autogenous shrinkage is the concrete shrinkage without loss of water. This shrinkage occurs as water is consumed in the hydration reaction. The majority of autogenous shrinkage occurs during the hydration process.

Concrete is prone to volumetric changes due to thermal and moisture related shrinkage at early ages. When there is restraint and concrete is prevented from shrinking freely, tensile stresses develop in the restrained concrete. Research performed by Khan, Murray et al. (2015) found that these tensile stresses induced by shrinkage are relaxed by creep. This makes it important to quantify the early-age tensile creep and shrinkage of concrete.

Shrinkage in composite bridges is important for serviceability as it affects both stress limitations and deflection. Alexander (2003) studied the effects of concrete shrinkage on composite steel beams. He found that shrinkage of the concrete slab has a direct and substantial effect on the deflection of steel girder bridges. Additionally, it was observed that shrinkage acts on the shear connectors in the opposite direction of loading.

Research on the effects of shrinkage on shrinkage induced deformations in composite steel and concrete bridges was also performed by Abdelmeguid (2016). This paper focuses on time dependent properties of shrinkage and creep in concrete being possible

causes for unwanted deflections in bridges. Two prototype beams with steel girders made composite with concrete deck slabs were built. The girders were W8x15 sections with a c/c span of 12 ft. The beams were designed to resemble the average tensile stresses in the concrete deck of the SH 86 bridge in Woods Co. Oklahoma. The beams were monitored for temperature, concrete strains, and deflections. Test results were compared to analytical models that focus on concrete shrinkage and temperature variations.

Concrete shrinkage in the range of 500 microstrains was observed from the laboratory testing. Theoretical mathematical models show that these shrinkage strains are sufficient to cause downward deflections in concrete decks made composite with steel beams. The prototype beams also exhibited slab shrinkage closely matching theoretical models assuming elastic behavior for the concrete deck. Theoretical models also predicted tensile stresses beyond 600 psi, which would cause the concrete slab to crack however, the prototype beams did not crack.

According to the results found in this paper, it is likely that problems related to the ride quality of bridges may be caused by volume changes in concrete bridge decks. From the results, it is suggested that the allowance for deflections due to shrinkage of concrete deck slabs be reduced from the current span/750. This paper also suggests that cracking may act as a relief for the restraining action of shrinkage strains on composite beams.

2.4 TEMPERATURE GRADIENTS IN COMPOSITE BRIDGES

Bridges are subjected to repeated cycles of heating and cooling from solar radiation and the surrounding air. For concrete-steel composite bridges, this exposure produces thermal movements and stresses in bridges due to external restraints and dissimilar material properties. These temperature-induced stresses depend on the end conditions of the bridge structure and the temperature distribution.

The current AASHTO LRFD Bridge Design Specifications provide temperature ranges to account for the overall expansion and contraction due to the presence of thermal changes through the depth of the structure. Figure 2.4 shows the temperature gradient provided by AASHTO. For the design temperature gradients, a map of the United States is divided in to four regions. For each region, a temperature T1 and T2 value is provided which defines the design positive temperature gradient. The values for these different regions is provided in Figure 2.5.

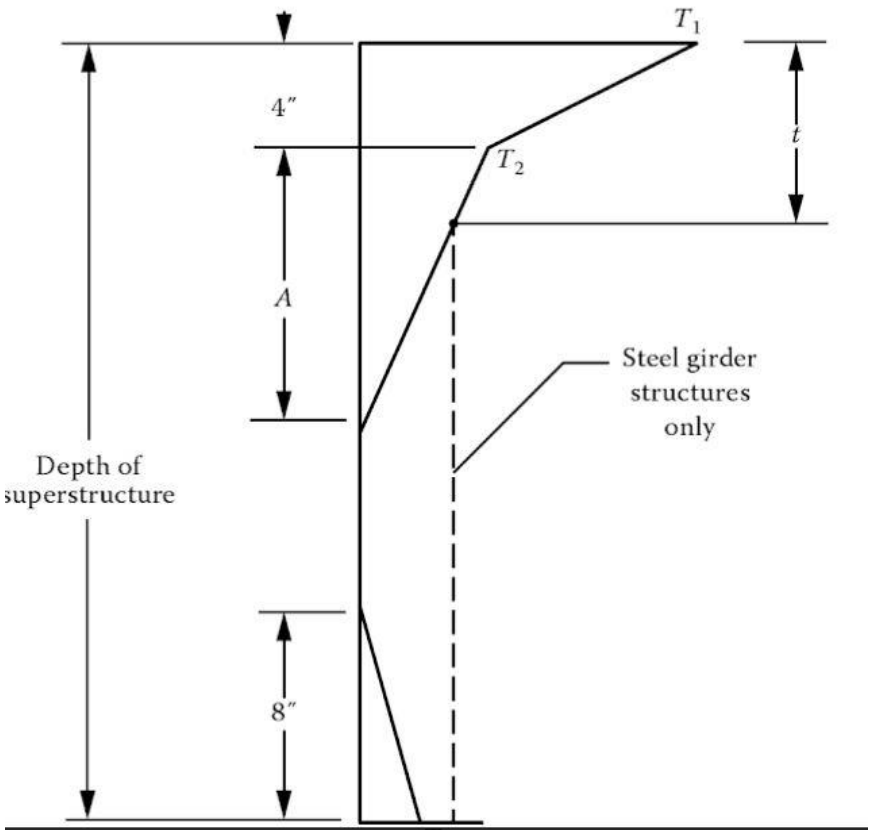

Figure 2.4: AASHTO Positive Vertical Temperature Gradient (Taly 2014)

TABLE 3.53
Basis for Temperature Gradients (AASHTO LRFD 2012 Table 3.12.3-1)

Zone	T_1 (°F)	T_2 (°F)
1	54	14
2	46	12
3	41	11
4	38	9

Figure 2.5: AASHTO Zone Basis for Temperature Gradients (Taly 2014)

Research performed by Krkoska and Moravcik (2017)monitored long-term temperature loading of a concrete box girder bridge beginning June 2015. The selected bridge has nine spans and was built using the incremental launching method with a 128 ft long steel

launching nose. The overall span of the bridge is 2739.8 ft with the main span crossing the highway and railway near Zilina airport. The superstructure consists of a continuous box girder simply supported by the piers and abutments. The depth of the cross-section varies between 12.6 ft and 14.8 ft. The concrete strength class was designed to C45/55 and prestressing tendons have a characteristic strength of 270 ksi. The tendons consist of 19 strands with bonded tendons and 27 strands with free tendons. Strand diameters are 0.62 in.

During construction, a total of 29 sensors were installed. Instrumentation used included 19 strain gages embedded in the concrete, 8 thermocouples to measure surface temperatures and 2 thermometers for measuring air temperatures. The sensors were divided into two cross-sections within the first span. All of the sensors were continually monitored and recorded.

The period of minimum temperatures for the research were reported. Temperature measurements throughout the structure exhibited a linear trend in the three portions of the beam: upper slab, web, and lower slab. The temperatures at the inner surface of the top slab were lower than the temperature inside the box. The temperature of the outer surface of the top slab was almost identical to the temperature of outside air. The temperature fields of the web was similar to that of the top slab except that the inner surface of the web was slightly higher than the temperature of outside air. For the bottom slab, the outer surface temperature was higher than the temperature of outside air creating a

negative temperature gradient in the cross section and the inner surface temperature was identical to the temperature inside the box.

The paper concluded that temperature gradients observed can exceed the value in bridge design standards. Krkoska states that it is necessary to collect specific temperature gradient data on various types of bridges to limit underestimating temperature gradients and allow for more precise structural analysis of bridge structures in the future.

Additionally, research by Rojas (2014) investigated the effects of temperature changes in concrete bridges. The thermal behavior of two bridges were monitored and compared to the established code design parameters. From this research, it was concluded that the maximum measured average bridge temperature gradients for both of the bridges monitored exceeded the service limit state established in the 2010 AASHTO LRFD Bridge Design Specifications.

Previous research by Fu, Ng et al. (1990) investigated the transient temperature and thermal stress distributions in various composite bridge structures. The effects of solar radiation and ambient temperature, material properties, and geometry on the distribution of temperature in a composite bridge were studied. From this research, it was found that the most influential variable on the temperature distribution was the slab overhang to depth ratio. This variable controls the area of the steel that is exposed to direct solar radiation. Additionally, Fu concluded that the convection constant substantially affected the temperature distribution. Possibly the most pertinent conclusion to this paper,

however, is that the daily air temperature extremes had a remarkable influence on the thermal behavior of a composite bridge.

CHAPTER III

STRAINS AND DEFLECTIONS IN COMPOSITE STEEL/CONCRETE BRIDGES AT EARLY AGES

3.1 INTRODUCTION

Concrete decks cast on steel bridge girders begin changing volume immediately upon taking initial set. Volume changes are caused as the concrete heats during curing, by drying shrinkage, and from creep. A large proportion of drying shrinkage occurs at early ages. This led some engineers in the Oklahoma DOT to theorize that concrete shrinkage is responsible for poor elevation control of concrete bridge decks that adversely affect ride quality. Additionally, after initial set, the volume changes are restrained by the steel girders, which may contribute to stresses that cause cracking in the concrete decks.

In our research, a full-scale prototype bridge was constructed from steel girders made composite with a concrete deck slab. The bridge was instrumented for concrete temperatures, steel temperature, concrete strains, steel strains, vertical deflections, and the angles of inclination of the steel beams at the supports. Results show downward deflections caused by the dead weight of the fresh concrete, unequal deflections of the formwork and bracing, elevated concrete temperatures at curing, upward deflections associated with elevated curing temperatures, and subsequent downward deflections and

concrete compressive strains consistent with concrete cooking and concrete shrinkage. This data was also used to observe the development of composite action.

Concrete cylinders were collected to establish material properties for the concrete, and included compressive strength, splitting cylinder tensile strength, elastic modulus, and coefficient of thermal expansion. Unrestrained shrinkage specimens were also cast to measure unrestrained shrinkage.

3.1.1 Research Objectives

- Observe the early age behavior of composite steel girder / concrete deck bridge systems and take measurements to determine the possible causes of unwanted deflections in steel/concrete composite bridges.
- Observe and measure beam and formwork deformations during construction of a full-sized prototypical steel girder bridge.
- Determine the short-term and near-term properties of concrete and relate those properties to the composite bridge behavior.
- Analyze strain data to determine the location of the neutral axis over time in early age setting and curing of the concrete slab, to determine the mechanisms and time after concrete deck casting when the bridge exhibits composite behavior.
- Determine causes for unwanted deformations in composite concrete/steel girder bridges.
- Make recommendations for new construction and rehabilitation of composite concrete/steel girder bridges.

3.2 BACKGROUND

Composite action exists when two different materials are bound together and act as a single unit. Composite action can be defined as occurring when strains in differing materials are equal at the boundary between those differing materials. In a composite concrete/steel girder bridge, composite action occurs when or where the strain at the bottom of the concrete slab equal the strain at the top of the steel flange. As the concrete deck hydrates and takes initial set, there is a partial interaction phase before achieving fully composite action (Azizinamini and Yakel 2006).

Minimal research has been conducted to determine when fully composite action occurs. Research by Subramaniam, Kunin et al. (2010) investigated the early age behaviors of composite steel girder concrete deck bridges due to the heat of hydration. In this research he observed that there was an increase in strain readings between the concrete deck and top of the steel flange 12 hrs. after slab cast. This phenomenon was related to the initial increase in temperature associated with the heat of hydration and is an indication that composite action has not yet occurred as the steel strain is different than that of the concrete. A decrease in strain followed this initial phenomenon that continued up to 48 hrs. after cast. It was also observed that during the first 48 hrs. of curing, there was large variation in the strain readings between the concrete deck and top of the steel flange indicating composite action has not yet set in. Beyond the 48 hrs., there was full strain compatibility between the deck and the top flange. This observation indicates that composite action has set in and the steel and concrete are now acting as a single unit.

Once the structure is composite, the concrete slab is restrained by the steel beam. Tensile stresses develop as drying shrinkage occurs in the concrete, however we do not know whether or not these stresses will cause cracking. Knowing when the bridge becomes composite will allow us to make necessary changes to construction practices in order to mitigate early age cracking of bridge decks.

Drying shrinkage is the result of water loss in hardened concrete. As a result of drying shrinkage, the hardened concrete changes in volume. Research by Abdelmeguid (2016) studied the deformations caused by shrinkage in composite steel and concrete bridges. His research showed that strains caused by drying shrinkage may account for some of the downward deflections in bridge decks. Despite the laboratory findings, investigations of real highway bridges found that shrinkage is not the likely cause of excessive deflections.

3.3 METHODOLOGY

3.3.1 Bridge Materials

A full-sized prototype bridge was constructed in the Bert Cooper Engineering Laboratory with two W24x94 girders made with A50 steel. Each girder is 39’-10” long, and spaced at 6 ft. center-to-center (c/c). The bridge replicates both the span and cross section dimensions from the Eagle Chief Creek Bridge “A” on SH 14 in Woods Co., OK. The actual bridge has a bridge deck measuring 30’-8” o/o supported by five W24x94 girders. Our full-sized prototype has two girders with an overall deck width of 14’-0”. The spans in both the SH14 Bridge in Woods Co. and the full-sized prototype match at 40’-0” nominal span with c/c of bearings spanning 38’-10”. The steel beams are supported by a pin at one end and a roller at the other. A photograph of the support conditions is

provided in Figure 3.1. Diaphragms are provided at mid-span as well as at the ends of the beams. The cross section details are shown in Figure 3.2.

Figure 3.1: Bridge Support Conditions

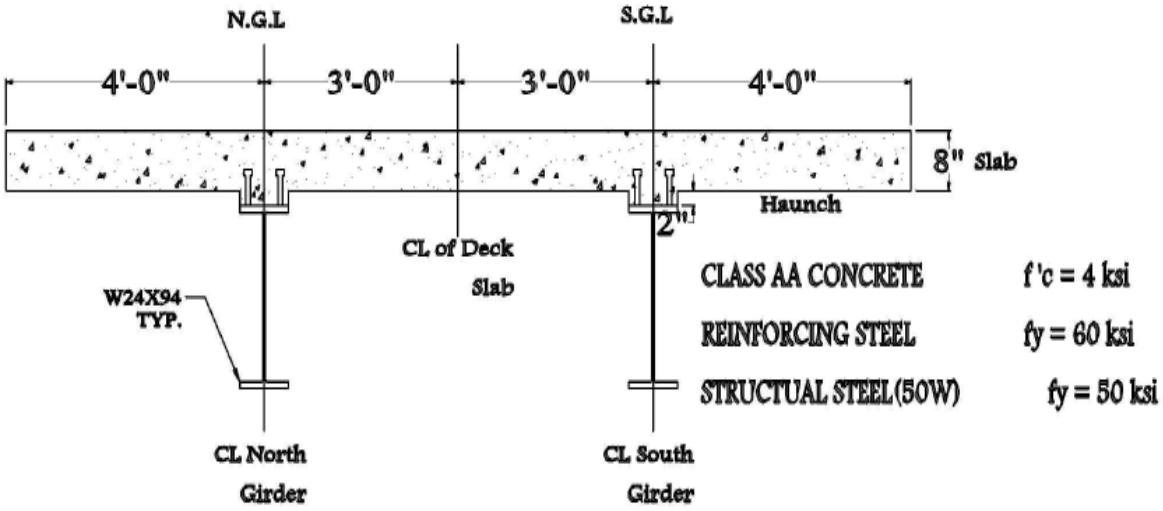

Figure 3.2: Cross-section drawing of composite bridge structure

The concrete mixture design conformed to the Class AA mixture of the Oklahoma DOT. The mixture proportions by weight for 1 CY of concrete are listed in Table 3.1. Cement conformed to ASTM C150, Type I/II. The aggregates were locally available crushed limestone and Guthrie sand provided by Dolese. The crushed limestone had a nominal aggregate size of ¾ in. Both the crushed limestone and the sand met ASTM C33 specifications. Aggregate properties can be found in Appendix 1. The concrete was batched locally and delivered in two trucks to the lab for placement. The trucks are labeled "Truck 1" and "Truck 2". Each truck was sampled twice for hardened properties and each sample is labeled "A" or "B".

Table 3.1: SSD Mixture Proportions

SSD MIXTURE PROPORTIONS		
	PCY	Volume (ft^3)
CEMENT	451	2.29
FLY ASH	113	0.68
QUAPAW 57	1845	10.56
GUTHRIE SAND	1362	8.30
WATER	28.5 gal	3.81
WRA	22.6 oz	
AEA	5 oz	
HRWRA	3.5 /c	
AIR	6 %	1.62

The concrete mixture targeted a 6% air content and was achieved using an air entrainment agent (AEA) from BASF. A slump of 7-8 in. was desired to ensure the workability and ease of placement needed for high quality concrete work. To achieve this slump without increasing the water content, a normal range and high range water reducing agent were used. Fresh concrete properties are provided in Table 3.2.

Table 3.2: Fresh Concrete Properties

FRESH CONCRETE PROPERTIES		
	Truck 1	Truck 2
SLUMP	9.5 in	8.25 in
UNIT WEIGHT	144.2 lb/ft^3	141.8 lb/ft^3
CONCRETE TEMPERATURE	91.5 ˚F	91.3 ˚F
TOTAL AIR CONTENT	8 %	9 %
OUTDOOR AMBIENT TEMPERATURE	92 ˚F	92 ˚F
INDOOR AMBIENT TEMPERATURE	74 ˚F	74 ˚F

Fresh property measurements were taken for both trucks. Tests performed included slump, unit weight and air content in accordance with ASTM C143-15a and ASTM C138-17a respectively. The temperature of the fresh concrete was also obtained. The average 28-day compressive strength expected from the ODOT AA concrete was 5,320 psi and was obtained from the Dolese strength performance report.

3.3.2 Slab Casting

Altogether, 14 CY of concrete were required for casting the concrete deck. The concrete volume was split evenly between two trucks, so seven cubic yards was supplied via each of the two trucks. The concrete deck was poured on July 13, 2017. The pour began at 11:10 am and concluded at 12:45 pm. The pour initiated at the west abutment and proceeded to the east abutment. The ambient temperature of the laboratory during casting was 74 °F. The process of casting the deck included consolidating, screeding, floating and finishing. Finishing of the surface was performed by Higgins Concrete and was completed at 1:40 pm. A broom finish was provided. Higgens Concrete is an external vendor that specializes in profession concrete finishing.

Figure 3.3 - Photograph of bridge slab (a) during cast (b) at 14 days after finishing and wet curing with burlap for 14 days

The deck slab was covered with wet burlap at 3:55 pm. Plastic was placed over the burlap to prevent the escape of moisture and water was applied to the burlap periodically after initial covering to ensure moist curing for a duration of 14 days after casting.

3.3.3 Specimen Preparations

Samples were taken from each truck to prepare specimens for shrinkage, coefficient of thermal expansion (CTE) and hardened property testing. A total of 118 cylinders and 6 shrinkage beams were made from the concrete used to make the bridge deck. Half of the specimens (59) were made from Truck 1 with the other half made from Truck 2. The specimens from each truck were also split by taking samples at two different times – one set beginning with each truck and a second set near the halfway point of each truck.

Cylinders were prepared in accordance with ASTM C172-17. Cylinders for hardened property testing were made using a standard 4 in. x 8 in. cylinder mold and the shrinkage beams were made using a standard 12 in. x 4 in. x 4 in. prism mold. After curing for 24 hrs. at the bridge deck, cylinder specimens were placed in the Cooper Lab curing room

which conforms to ASTM C192 curing requirements. Shrinkage specimens were covered with wet burlap and kept near the bridge deck for a duration of 14 days. After the 14 days of curing, shrinkage specimens were placed in a climate controlled room with a temperature of 72 °F and a relative humidity of 50%. Target Points for the Detachable Mechanical Strain Gage (DEMEC points) were applied to the shrinkage specimens after the first 24 hrs. of curing to measure shrinkage strains.

3.3.4 Instrumentation and Data Acquisition

Before casting of the concrete, approximately 100 electronic instruments were installed onto the bridge. The instruments used included the following:

- Bonded Foil Strain Gages (electronic resistance strain gages). These were applied to the steel girders and were used to measure strains in the steel girders. They were also applied to the concrete deck slab surfaces after the slab was cast, and after wet curing.
- Vibrating Wire Strain Gages (VWSG) were placed at various locations within the concrete slab.
- Thermocouples. There are five sets of thermocouples. Each set consists of five individual thermocouples for a total of 25 installed. These were placed at five locations in the slab. Within each set, the five thermocouples are positioned at varying depths within the slab in order to measure the concrete temperature within the slab. The positioning of the thermocouples allowed us to capture thermal gradients within the slab.

- Linear Voltage Displacement Transducers (LVDTs). These were placed at strategic locations to measure deflections of the beams and slab.
- Inclinometers. One inclinometer was placed at each end of each steel girder. From these, we can capture the angle change at the ends of the girders. Many researchers are using inclinometers at end regions in place of direct deflection measurements in structural health monitoring.
- Displacement gages. Several visual displacement gages were placed at key locations around the bridge in order to obtain manual displacement readings.
- Target Points for the Detachable Mechanical Strain Gage (DEMEC points) were applied to the steel girder to provide a manual measurement of steel girder strains prior to, during, and after slab casting.

Readings were recorded every 5 minutes for the first 28 days after bridge cast and then transitioned to every 30 minutes. All of the electronic instrumentation was recorded to a data logger that helped electronically interpret the data, which then fed to a computer for storage of the data.

Figure 3.4 - Photograph of thermocouples used for data collection: Thermocouples were placed at the top and bottom surface of the deck and at 2in., 4in., and 6in. depths.

Figure 3.5 - Photographs of VWSG used for data collection: VWSG were placed at 2 in., 4 in. and 6in. depths.

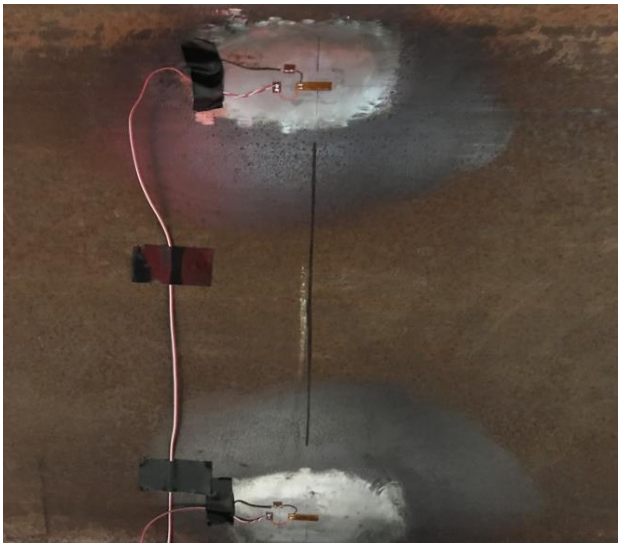

Figure 3.6 - Photograph of bond foil strain gages used for data collection: The strain gages were placed 4 in. above the bottom flange and 4 in. below the top flange at the mid-span of the girder.

3.3.5 Materials Testing

3.3.5.1 Fresh Properties

Fresh property measurements were taken for both trucks. Tests performed included slump, unit weight and air content in accordance with ASTM C143-15a and ASTM C138-17a respectively. The temperature of the fresh concrete was also obtained. 5 gallons of water were added to the second truck at the laboratory before casting so that the slump would be consistent with the first truck. The w/cm was gaged with the amount of slump we measured.

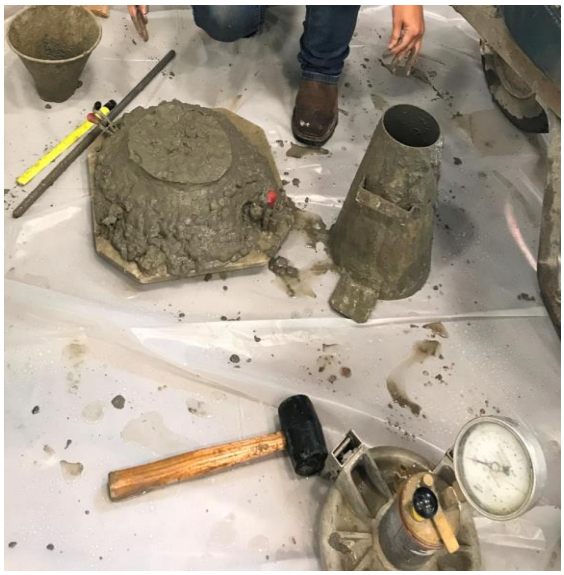

Figure 3.7 - Performing slump test on bridge deck concrete

3.3.5.2 Hardened Properties

Concrete compressive strengths were obtained at 1 d, 3 d, 7 d, 14 d, and 28 d in accordance with ASTM C39-18. Elastic modulus and splitting tensile strengths were measured in accordance with ASTM C469-14 and ASTM C496-17 respectively, and values were obtained at 1 d, 3 d, 7 d, and 28 d. Hardened concrete properties are presented in Tables 3.3-5.

3.4 RESULTS & DISCUSSION

3.4.1 Concrete Properties

3.4.1.1 Hardened Concrete Properties

The results for compressive strength, elastic modulus, and tensile strength for the first 28 days are listed in Table 3.3, 3.4, and 3.5 respectively. Two trucks delivered concrete for the bridge deck; data is segregated by truck.

Table 3.3: Measured Compressive Strength

COMPRESSIVE STRENGTH, C39 (PSI)						
SAMPLE	1 day	3 day	7 day	14 day	21 day	28 day
1A	1410	3260	4040	4570	4880	4960
1B	1560	3620	4350	4810	5200	5530
TRUCK 1 AVERAGE	**1485**	**3440**	**4195**	**4690**	**5040**	**5245**
2A	2250	4090	4660	5310	5550	5800
2B	1940	3640	4270	4980	4880	5400
TRUCK 2 AVERAGE	**2095**	**3865**	**4465**	**5145**	**5215**	**5600**

Table 3.4 Measured and Calculated Elastic Modulus

ELASTIC MODULUS, C469 (KSI)				
SAMPLE	1 Day	3 Day	7 Day	28 Day
1A	574 (a)	3020	3350	3650
1B	2620	3090	3400	4030
TRUCK 1 AVERAGE	**2620**	**3055**	**3375**	**3840**
TRUCK 1 CALCULATED (b)	***2220***	***3380***	***3730***	***4170***
2A	2580	3600	4160	4180
2B	2230	3110	3390	3880
TRUCK 2 AVERAGE	**2405**	**3355**	**3775**	**4030**
TRUCK 2 CALCULATED	***2640***	***3580***	***3850***	***4310***

NOTES:
(a): there is error in this value therefore it is disregarded in the truck 1 average.
(b): the "calculated" elastic modulus comes from aci eqn. 19.2.2.1.a –
ec = 33w^1.5*sqrt(f'c)

Table 3.5 Measured and Calculated Splitting Tensile Strength

TENSILE STRENGTH, C496 (PSI)				
SAMPLE	1 Day	3 Day	7 Day	28 Day
1A	128(a)	375	498	564
1B	217	446	525	518
TRUCK 1 AVERAGE	**217**	**411**	**512**	**541**
TRUCK 1 CALCULATED (a)	***231***	***352***	***389***	***435***
2A	318	524	667	648
2B	360	371	509	555
TRUCK 2 AVERAGE	**339**	**447**	**588**	**602**
TRUCK 2 CALCULATED	***275***	***373***	***401***	***449***

NOTES:
(a): there is error in this value therefore it is disregarded in the truck 1 average.
(b): The "calculated" tensile strength comes from ACI Eqn. 19.2.4.3- fct = 6.7*sqrt(f'c)

The testing of cylinders made from the bridge deck mixture resulted in an average 28-day compressive strength of 5,423 psi. The data on elastic modulus indicated that the engineering formulae generally used for elastic modulus slightly over-predicts E for these materials.

3.4.1.2 Concrete Prism Shrinkage Strains

The unrestrained concrete shrinkage strains recorded from the concrete prisms made during casting are represented in Figure 3.8. These measurements were taken using DEMEC points on the top surface of the concrete prisms. It is noticed that there is a difference between the shrinkage of the unrestrained concrete prisms and the shrinkage in the deck slab. This indicates that the steel is restraining expansion and contraction in the deck slab.

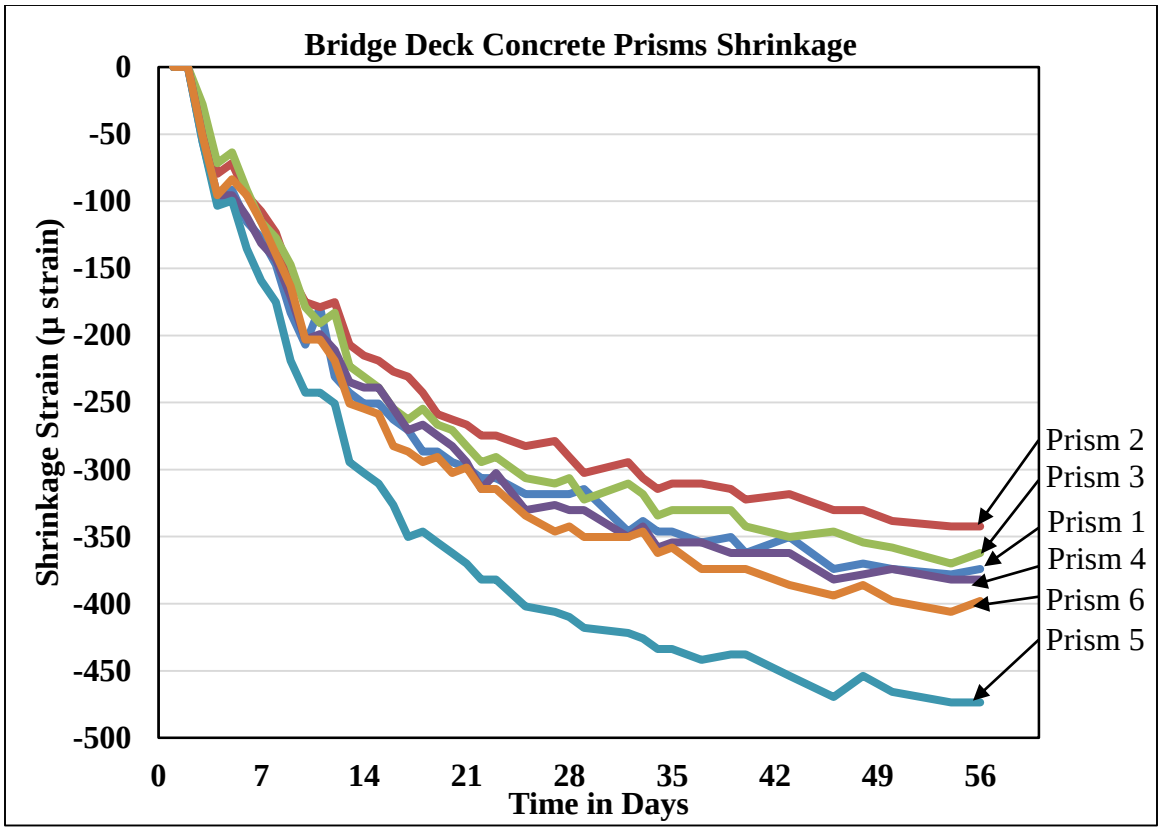

Figure 3.8 - Bridge Deck Concrete Prism Strains: Concrete prism unrestrained shrinkage strains were measured using DMEC points on 6 prisms made at casting. The average strain after 56 days was approximately 380 µ strain.

3.4.2 Bridge Deck Deflections

The deflections were measured at mid-span of the bridge at four locations: the bottom side of both steel girders and the bottom side at the edges of the concrete slab overhang. The locations of the LVDTs used for measurement deflections are shown in Figure 3.9.

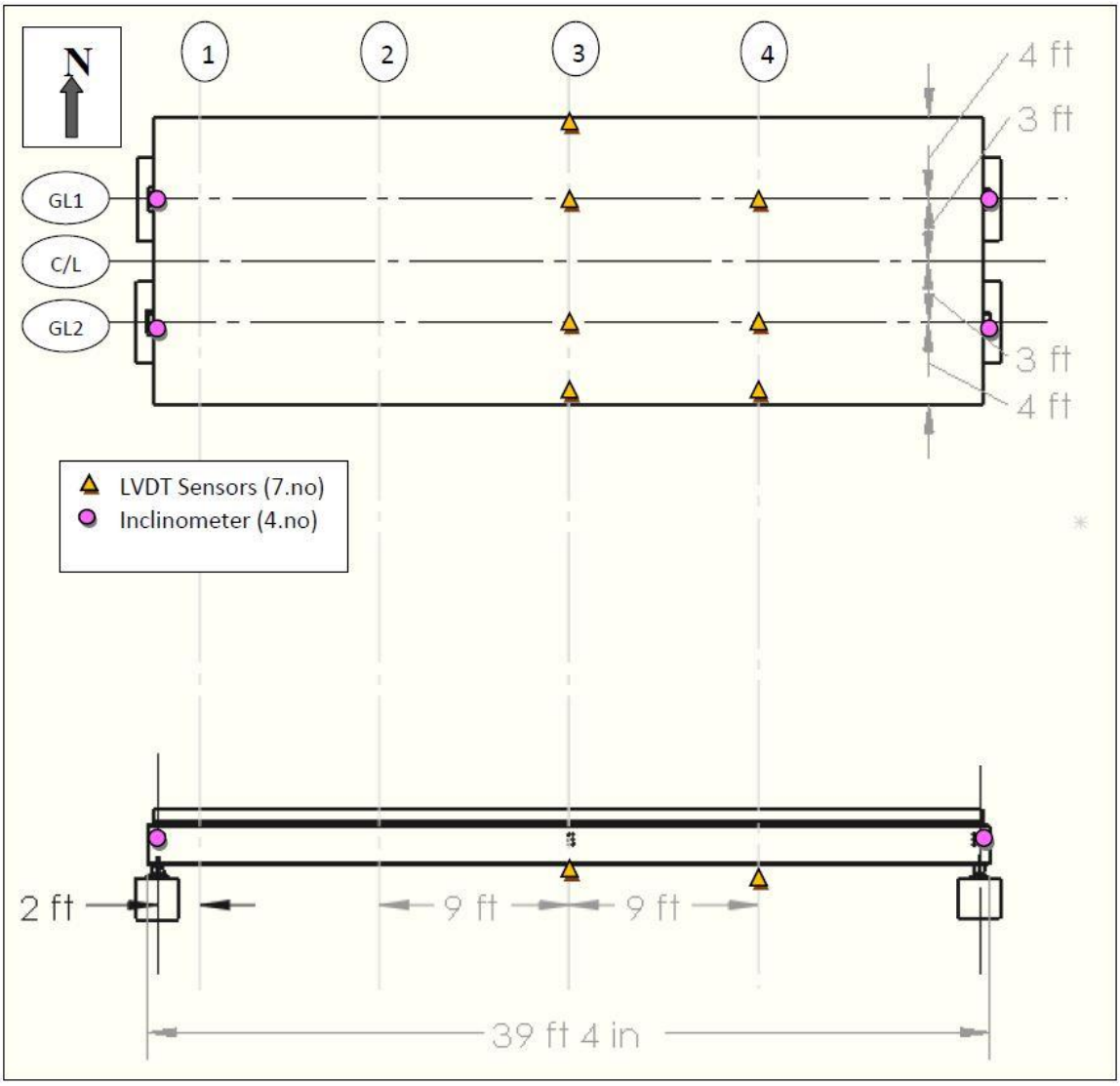

Figure 3.9: Locations of LVDTS

3.4.2.1 Mid-Span Deflections 24 Hours After Deck Cast

Deflections of the steel girders and concrete overhang were measured immediately before deck pour, as the deck was cast and immediately after the deck was cast. Results for the first 24 hrs. after the start of casting are shown in Figure 3.10. It can be seen that the steel girders deflected approximately 0.40 in under the dead load of the fresh concrete. The concrete overhang deflected an additional 0.45 in beyond that of the steel girders.

The additional deflections in the overhang are considered to be excessive and are a result of inadequate bracing during construction.

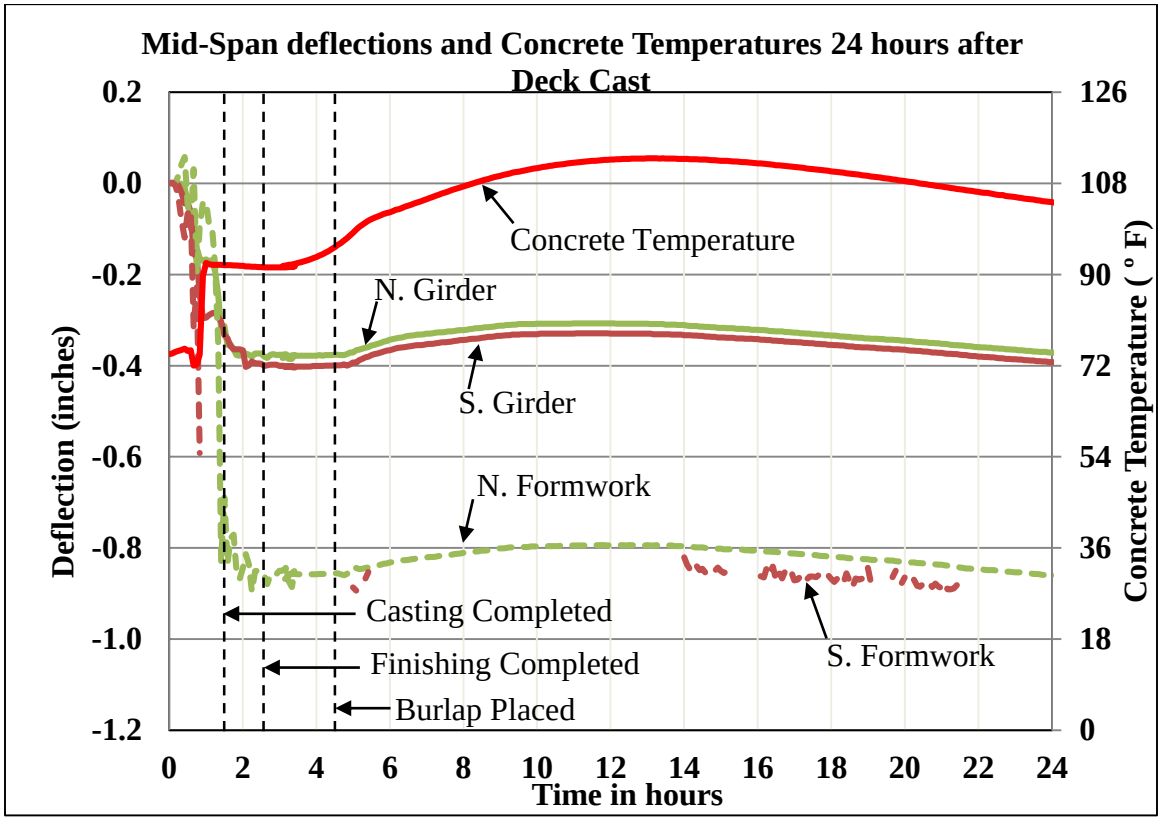

Figure 3.10- Mid-Span deflections 24 hrs. after deck cast: Deflections are measured at mid-span using LVDTs and the temperature was measured with thermocouples. The maximum temperature experienced was 114 °F and occurred about 13 hrs. after slab cast.

Figure 3.10 shows the concrete deck temperature plotted over time with the vertical deflection of the bridge girder. Deflections are measured at four locations: deflections at mid-span of both the north and south steel beams, and the deflections at the north and south edges of the concrete deck slab, also at mid-span. The data show initial downward deflection that corresponds with casting of the concrete and the addition of dead load caused by the weight of the fresh concrete. Then upward deflections are noted from approximately 3 hrs. to 12 hrs. which correspond with elevated temperatures in the bridge

deck caused during hydration. After 12 hrs. the concrete deck begins to cool and the deflections observed go downward. The agreement in upward deflections between the steel girders and concrete deck indicate that there exists some degree of composite action occurring in the bridge.

3.4.2.2 Mid-Span Deflections 28 Days After Deck Cast

The overall beam deflections measured for the first 28 days are illustrated in Figure 3.11. The data labeled "N. Formwork" and "S. Formwork" were adjusted to formwork thickness after the formwork was removed and measured directly to the bottom of the deck slab.

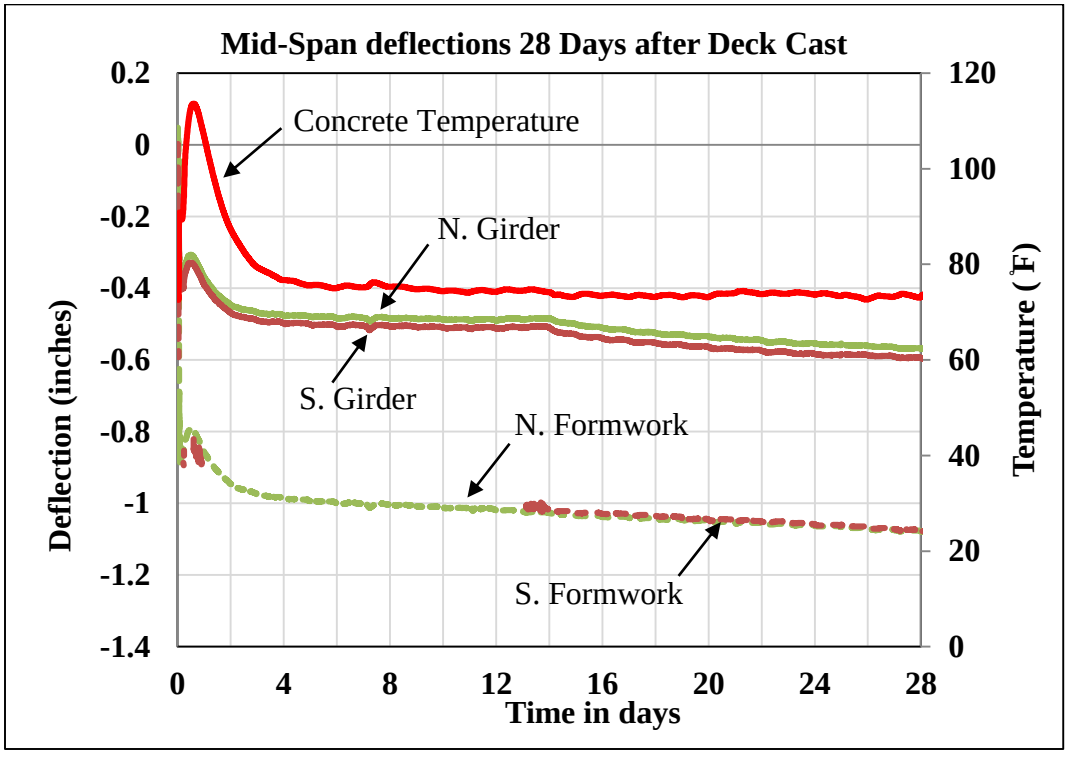

Figure 3.11 - Mid-Span Deflections 28 Days After Deck Cast: Deflections are measured at mid-span using LVDTs and the temperature was measured with thermocouples. After 28 days the temperature and girders deflections leveled out to approximately 73 °F and -0.6 in. respectively.

Figure 3.11 shows the concrete deck temperature plotted over time with the vertical deflection of the bridge girders and concrete deck slab. Deflections are measured at four locations: deflections at mid-span of both the north and south steel beams, and the deflections at the north and south edges of the concrete deck slab. Over the span of 28 days from casting, it is noticed that the bridge deflected an additional 0.192 in downward beyond the initial deflection of 0.40 and 0.85 of the girder and formwork respectively due to the dead load from the concrete. This additional increase in downward deflections indicates that concrete shrinkage is affecting the behavior of the composite bridge, and that volume changes in the concrete deck are likely causing the downward deflections. A difference in deflection of approximately 0.45 in between the steel and edge of slab that occurred during casting of the deck remained constant during the 28 days after casting.

3.4.3 Bridge Deck Strains

Concrete strains were taken at depths of 2 in., 4 in., and 6 in. from the bottom of the concrete deck slab. Bottom steel strains were measured 4 in. above the top of the bottom flange and 4 in. below the bottom of the top flange.

3.4.3.1 Mid-Span Strains 72 Hours After Deck Cast

The strains and temperatures of the concrete deck are presented in Figure 3.12. As the concrete temperature changed during the hydration process, the change in strains in the concrete followed a pattern similar to that of the change in temperature.

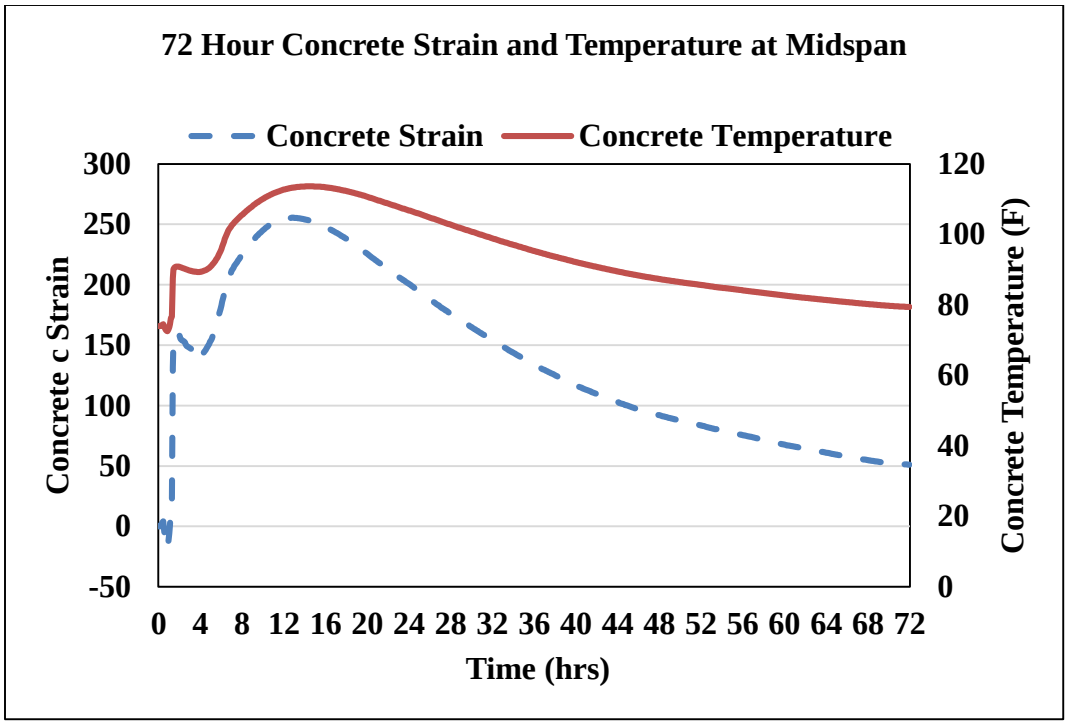

Figure 3.12 - Concrete Mid-Span Strain and Temperature 72 Hrs After Deck Cast: Strain and temperature were measured using a VWSG 2 in. from the bottom of the slab. A maximum hydration temperature of 114 °F was reached approximately 14 hrs. after casting with a corresponding strain of approximately 240 μ strain.

Figure 3.12 shows the concrete deck temperature plotted over time with the corresponding concrete strain at mid-span. Strain and temperature were both measured using a VWSG and was located 2 in. from the bottom of the slab at mid-span of the deck. It is observed that at approximately 14 hrs. after the start of slab casting, the heat of hydration reaches a maximum value of 114 °F. After the 14-hr. mark, the temperature began to gradually decrease as well as the strains. The maximum tensile strain reached in the concrete was approximately 240 μ strain.

3.4.3.2 Mid-Span Strains 28 Days After Deck Cast

Figure 3.13 shows the concrete temperatures and strains measured over time for the first 28 days after deck casting. The chart shows elevated concrete temperatures in the first 24 hrs., followed by falling temperatures as the concrete deck gradually returns to ambient temperature conditions. As the concrete reaches this ambient temperature condition, concrete compressive strains continued to increase with the likely cause being concrete shrinkage.

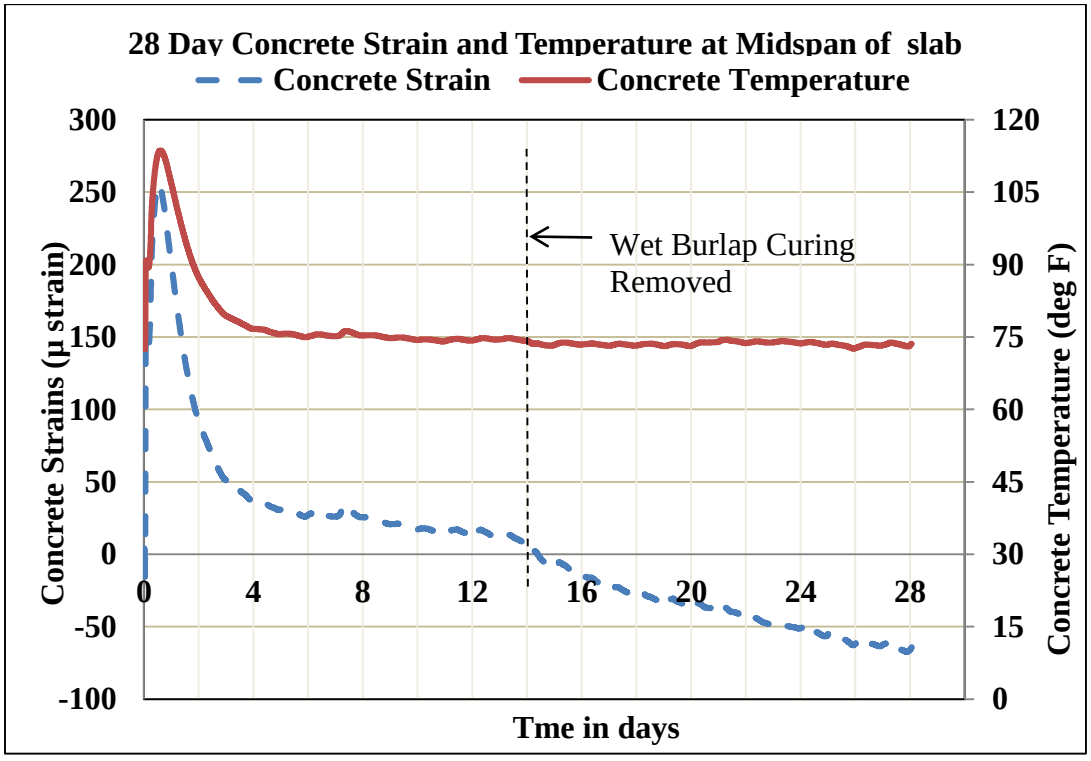

Figure 3.13 - Concrete Mid-Span Strain and Temperature 28 Days After Deck Cast: Wet burlap curing was removed 14 days after slab cast. Concrete temperatures leveled out to approximately 73 °F. Restrained shrinkage strains continue to increase over time.

Figure 3.14 shows the concrete strains measured over time from the beginning of deck casting through 28 days. At the mid-span location of the slab, three vibrating wires were installed prior to concrete pour to capture the strain gradient throughout the depth of the

slab. The concrete compressive strains continued to increase with the most likely cause being concrete shrinkage. This restrained concrete shrinkage strain continued to increase over time and was found to be larger near the top surface of the deck.

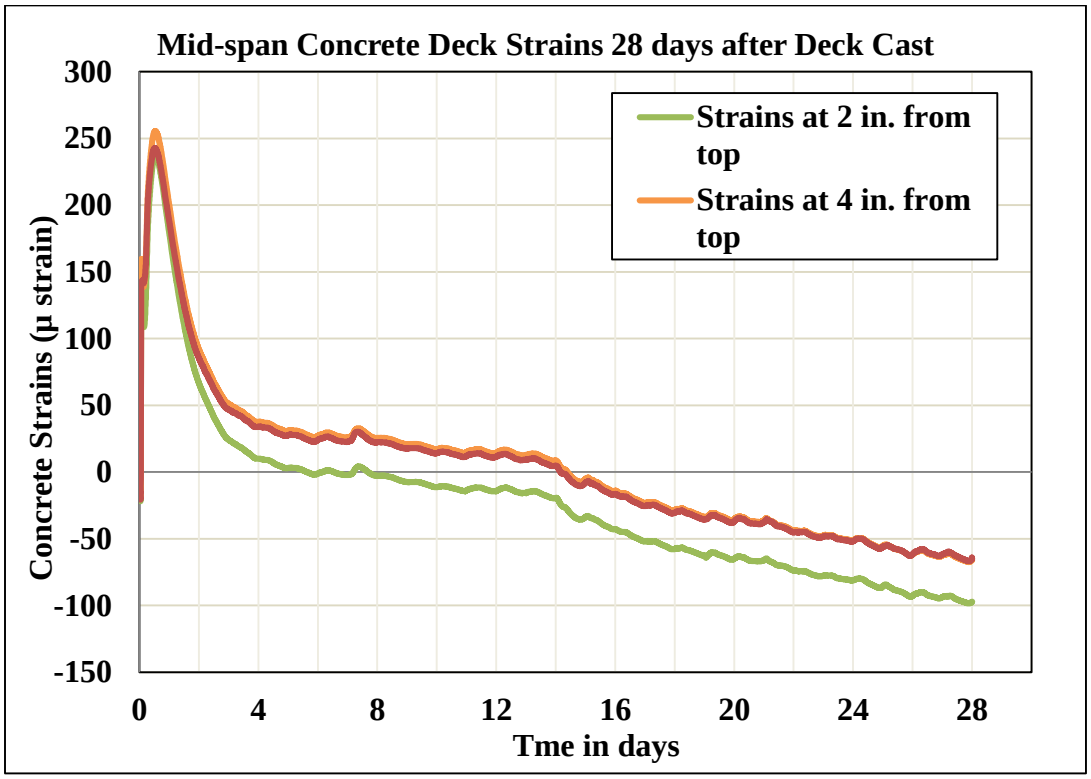

Figure 3.14 - Concrete Mid-Span Strains 28 Days After Deck Cast: Strains were measured using VWSG at depths of 2, 4, and 6 in. from the top of the deck slab. Restrained concrete shrinkage strains reached a maximum of 250 μ strain after 14 hrs. and then continually decreased. Strains were found to be larger near the top surface of the deck.

Strains in the steel girders at mid-span are presented in Figure 3.15. It is seen that there is very little variation in the strains in the North and South girders for the duration of the 28 days.

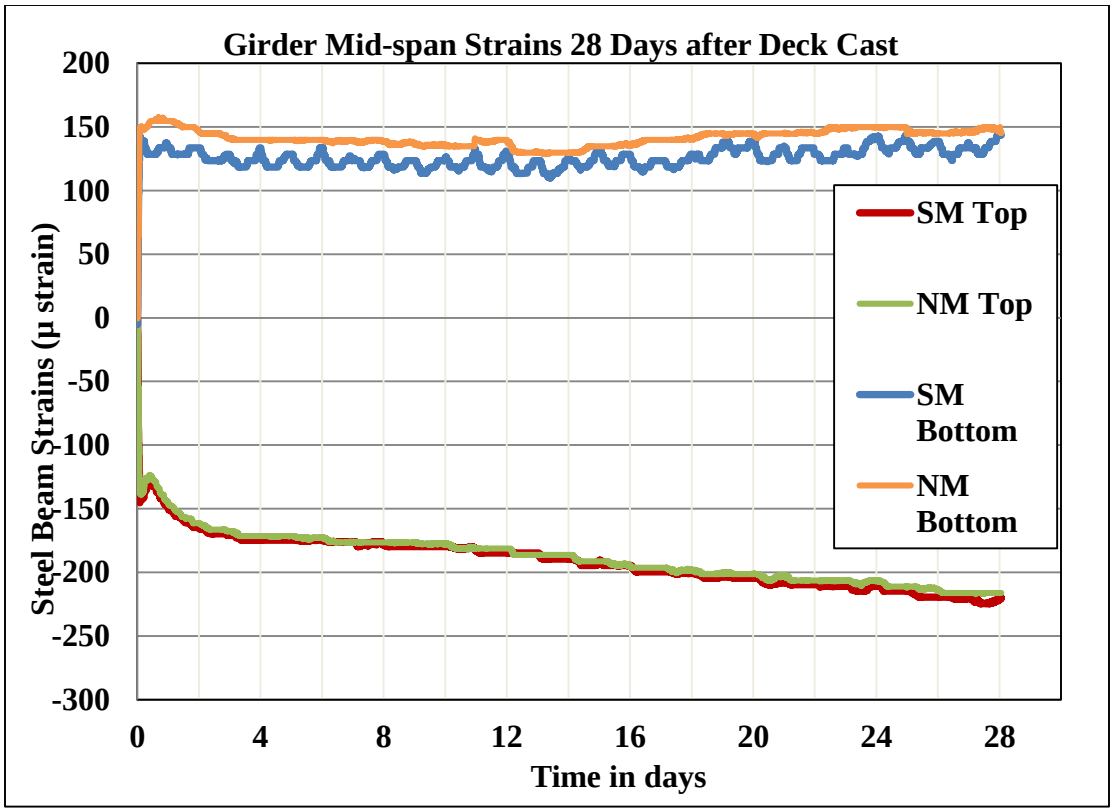

Figure 3.15 - Girder Mid-Span Strains 28 Days After Deck Cast: Steel strains were measured using Bonded Foil Strain Gages 4 in. from the top and bottom of the girder at mid-span. There was little variation between the North and South girders. Strains gradually continue to increase over time.

3.5 CONCLUSION

From the analysis of the data, the following conclusions can be drawn:

- Measured deflections caused by the self-weight of the concrete was 0.38 in. and 0.40 in. on the two girders. The nearly matches the deflections computed using beam theory, a span of 38.83 ft. and a unit weight of concrete of 150 pcf, which yielded a calculated deflection of
- Deflections in the concrete overhang were 0.45 in. more than the deflection of the girders.

- Further research is needed to design a more adequate bracing system to reduce initial deflections.
- Further research should be performed to determine the influence of creep on early age deflections.
- The bridge deflected upward approximately 0.08 in. due to the heat of hydration of the concrete deck, which also proves composite action.
- The bridge deflected downward as the deck cooled.
- Shrinkage of the concrete deck increased after the wet curing was removed at 14 days. Also, the bridge's downward deflection accelerated after the wet curing was removed indicating a correlation between slab shrinkage and downward deflection of the bridge.

CHAPTER IV

RADIANT HEATING OF CONCRETE BRIDGE DECKS AND ITS EFFECTS ON BRIDGE DEFLECTIONS, STRAINS, AND DEFORMATIONS

4.1 INTRODUCTION

Concrete bridge decks are subject to repeated temperature changes that cause temperature gradients through the depth of the slab. These temperature gradients produce internal thermal stresses that result directly in bridge deformations. The volume changes in concrete due to these temperature changes cause upward and downward bridge deflections, differential strains, and internal stresses within the concrete deck. The combined effect of these phenomena can adversely affect the ride quality, cause deck cracking and excessive deflections, decrease durability, and reduce long-term performance of steel girder bridges made composite with concrete decks. The goal of this project is to examine the effects of thermal strains and stresses caused by regular and repeated heating of concrete bridge decks, and to determine what effect thermal stresses and strains may have on performance of steel girder bridges made composite with concrete decks.

In our research, a prototype bridge was constructed from steel girders made composite with a concrete deck slab. Thermal loads up to 120 °F were applied to the bridge deck by an array of heat lamps. A temperature of 120 °F was targeted to resemble summer time

temperatures in Oklahoma. The bridge was monitored for temperature, concrete strains, steel strains, and deflections. From the gathered data, the temperature gradient through the concrete slab was found and compared to the current AASHTO temperature gradient to determine if the temperature induced stresses meet the code limitations. Data collected was also used to assess the deflections and strains caused by the thermal loading.

Concrete cylinders were collected to establish material properties for the concrete to include compressive strength, tensile strength, and elastic modulus. Unrestrained shrinkage specimens were also cast to measure unrestrained shrinkage.

4.1.1 Research Objectives

- Determine the deflections caused in bridge decks due to thermal loading.
- Monitor temperature gradient throughout the depth of the concrete and steel during temperature load testing and compare the observed temperature gradient from the prototype bridge to the AASHTO temperature gradient to determine if temperature induced stresses meet code limitations.
- Determine the effects on short term deflections, incidence of cracking and composite action between steel girders and concrete decks.

4.2 BACKGROUND

Varying temperature distributions through bridge depths result in flexural deformations while uniform temperature changes through the depth cause axial deformations (Reynolds 1972). When the thermal expansion or contraction of concrete is restrained, solar radiation and the daily temperature variations it causes, will result in thermal

stresses and a temperature differential throughout the section (Imbsen, Vandershaf et al. 1985, Hadidi, Saadeghvaziri et al. 2003, El-Tayeb, El-Metwally et al. 2017, Krkoska and Moravcik 2017). There are many factors affecting temperature variations such as the difference between the construction temperature and the maximum or minimum temperatures in the summer and winter and the geometry and dimensions of the bridge (Rodriguez, Barr et al. 2014, El-Tayeb, El-Metwally et al. 2017).

The temperature variations caused by thermal loads in the bridge superstructure are referred to as the temperature gradient. Current AASHTO specifications provide probable temperature ranges that should be considered in the design process based on the location of the bridge. It has been found that the temperature gradients due to these thermal loads exceed the design values provided in bridge design standards (Krkoska and Moravcik 2017). In addition, severe cracking and deterioration have been the result of imprecise thermal analysis of bridges (Rodriguez, Barr et al. 2014).

Increasing amounts of research are showing that cracks in bridge decks at early ages may be caused by the restrained deformation of concrete in relation to thermal and shrinkage effects and not directly related to the external loading (Subramaniam, Kunin et al. 2010). While there have been numerous studies on the relation between deck cracking and restrained shrinkage, fewer studies have been performed to determine the relationship between temperature changes and cracking. The presence of strain due to creep and shrinkage further complicates the study and analysis of thermals strains.

4.3 METHODOLOGY

4.3.1 Bridge Materials

A full-sized prototype bridge was constructed in the Bert Cooper Engineering Laboratory with two W24x94 girders made with A50 steel. Each girder is 39’-10” long, and spaced at 6 ft. center-to-center (c/c). The bridge replicates both the span and cross section dimensions from the Eagle Chief Creek Bridge “A” on SH 14 in Woods Co., OK. The actual bridge has a bridge deck measuring 36’-0” o/o supported by five W24x94 girders. Our full-sized prototype has two girders with an overall deck width of 14’-0”. The spans in both the SH14 Bridge in Woods Co. and the full-sized prototype match at 40’-0” nominal span with c/c of bearings spanning 38’-10”. The steel beams are supported by a pin at one end and a roller at the other. A photograph of the support conditions is provided in Figure 4.1. Diaphragms are provided at mid-span as well as at the ends of the beams. The cross section details are shown in Figure 4.2.

Figure 4.1: Bridge Support Conditions

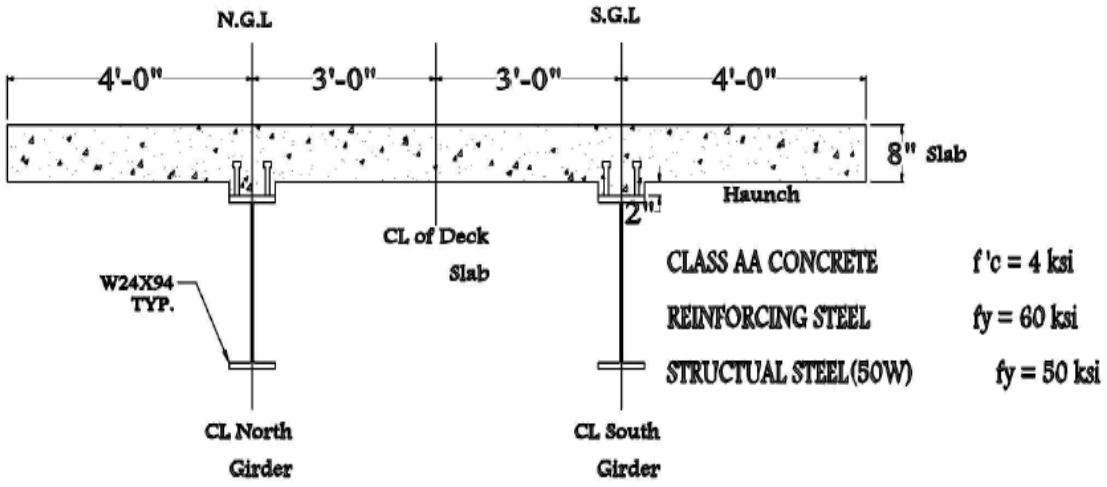

Figure 4.2: Cross-section drawing of composite bridge structure

The concrete mixture design conformed to the Class AA mixture of the Oklahoma DOT. The mixture proportions are listed in Table 4.1. Cement conformed to ASTM C150, Type I/II. Fly ash was a Type C. The aggregates were locally available Quapaw #57 crushed limestone and Guthrie sand provided by Dolese. The crushed limestone had a nominal aggregate size of ¾ in. Both the crushed limestone and the sand met ASTM C33 specifications. Aggregate properties can be found in Appendix 1. The concrete was batched locally and delivered in two trucks to the lab for placement. The trucks are labeled "Truck 1" and "Truck 2". Each truck was sampled twice for hardened properties and each sample is labeled "A" or "B".

Table 4.1: SSD Mixture Proportions

SSD MIXTURE PROPORTIONS		
CEMENT	450	lb/yd^3
FLY ASH	114	lb/yd^3
QUAPAW 57	1854	lb/yd^3
GUTHRIE SAND	1335	lb/yd^3
WATER	29.5	lb/yd^3
WRA	22.6	oz
AEA	5	oz
HRWRA	3.5	/c
AIR	6	%

The concrete mixture targeted a 6% air content and was achieved using an air entrainment agent (AEA) from BASF. A slump of 7-8 in. was desired to ensure the workability and ease of placement needed for high quality concrete work. To achieve this slump without increasing the water content, both normal range and high range water reducing agents were used. The average 28-day compressive strength expected from the ODOT AA concrete was 5,370 psi and was obtained from the Dolese strength performance report. The testing of cylinders made from the bridge deck mixture resulted in an average 28-day compressive strength of 5,423 psi.

4.3.2 Slab Casting

Altogether, 14 CY of concrete were required for casting the concrete deck. The concrete volume was split equally between two trucks, so seven cubic yards were supplied via each of the two trucks. The concrete deck was cast on July 13, 2017. The placement began at 11:10 am and concluded at 12:45 pm. The pour initiated at the west abutment and proceeded to the east abutment. The ambient temperature of the laboratory during casting was 74 °F. The process of casting the deck included consolidating, screeding,

floating and finishing. Finishing of the surface was performed by Higgins Concrete and was completed at 1:40 pm. A broom finish was provided. Higgins Concrete is an external vendor that specializes in professional concrete finishing.

Figure 4.3: Photograph of bridge slab (a) during cast (b) at 14 days after finishing and wet curing with burlap for 14 days

The deck slab was covered with wet burlap at 3:55 pm. Plastic was placed over the burlap to prevent the escape of moisture and water was applied to the burlap periodically after initial covering to ensure moist curing for a duration of 14 days after casting.

4.3.3 Concrete Material Specimen Preparations

Samples were taken from each truck to prepare specimens for shrinkage and hardened property testing. A total of 118 cylinders and 6 shrinkage beams were made from the concrete used to make the bridge deck. Half of the specimens (59) were made from Truck 1 with the other half made from the Truck 2. The specimens from each truck were also split by taking samples at two different times – one set beginning with each Truck and a second set near the halfway point of each truck.

Cylinders were prepared in accordance with ASTM C172-17. Cylinders for hardened property testing were made using standard 4 in. x 8 in. cylinder molds. Shrinkage beams were made using standard 12 in. x 4 in. x 4 in. prism molds. After curing for 24 hrs. near the bridge deck, cylinder specimens were placed in the Cooper Lab curing room which conforms to ASTM C192 curing requirements. Shrinkage specimens were covered with wet burlap and kept near the bridge deck for a duration of 14 days. After the 14 days of curing, shrinkage specimens were placed in a climate controlled room with a temperature of 72 °F and a relative humidity of 50%. Target Points for the Detachable Mechanical Strain Gage (DEMEC points) were applied to the shrinkage specimens after the first 24 hrs. of curing to measure shrinkage strains.

4.3.4 Instrumentation and Data Acquisition

Before casting of the concrete, approximately 100 electronic instruments were installed onto the bridge. The instruments included the following:

- Bonded Foil Strain Gages (electronic resistance strain gages). These were applied to the steel girders and were used to measure strains in the steel girders. They were also applied to the concrete deck slab surfaces after the slab was cast, and after wet curing.
- Vibrating Wire Strain Gages (VWSG) were placed at various locations within the concrete slab prior to slab casting.
- Thermocouples. There are five sets of thermocouples. Each set consists of five individual thermocouples for a total of 25 installed. These were placed at five locations in the slab. Within each set, the five thermocouples are positioned at

varying depths within the slab in order to measure the concrete temperature within the slab. The positioning of the thermocouples allowed us to capture thermal gradients within the slab.

- Linear Voltage Displacement Transducers (LVDTs). These were placed at strategic locations to measure deflections of the beams and slab.
- Inclinometers. One inclinometer was placed at each end of each steel girder. From these, we can capture the angle change at the ends of the girders. Many researchers are using inclinometers at end regions in place of direct deflection measurements in structural health monitoring.
- Displacement gages. Several visual displacement gages were placed at key locations around the bridge in order to obtain manual displacement readings.
- Target Points for the Detachable Mechanical Strain Gage (DEMEC points) were applied to the steel girder to provide a manual measurement of steel girder strains prior to, during, and after slab casting.

All of the electronic instrumentation was recorded to a data logger that helped electronically interpret the data, which then fed to a computer for storage of the data.

Figure 4.4 - Photograph of thermocouples used for data collection: Thermocouples were placed at the top and bottom surfaces of the deck and at depths of 2 in., 4 in., and 6 in.

Figure 4.5 - Photographs of VWSG used for data collection: VWSG were placed at depths of 2 in., 4 in. and 6in. prior to slab casting.

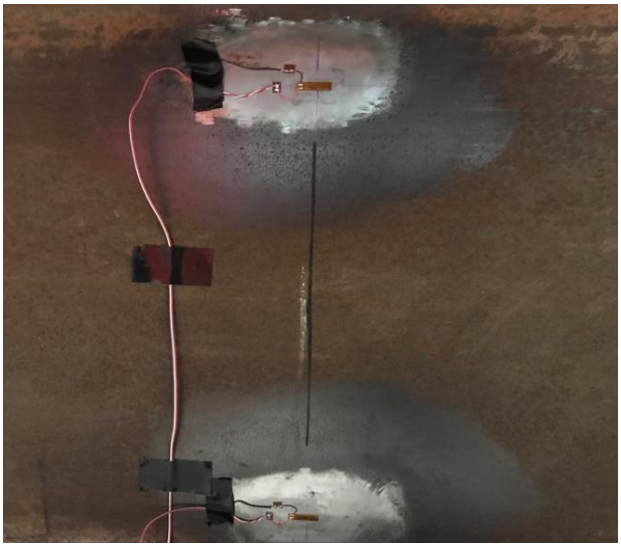

Figure 4.6 - Photograph of bond foil strain gages used for data collection: The strain gages were placed 4 in. above the top of the bottom flange and 4 in. below the bottom of the top flange at the mid-span of the girder.

4.3.5 Materials Testing

4.3.5.1 Fresh Concrete Properties

Fresh concrete properties were measured for both trucks, and included measurements for slump, unit weight and air content in accordance with ASTM C143-15a and ASTM C138-17a respectively. The temperature of the fresh concrete was also obtained. Fresh concrete properties are presented in Table 4.2. 5 gallons of water were added to the second truck at the laboratory before casting so that the slump would be consistent with the first truck. The w/cm was gaged with the amount of slump we measured.

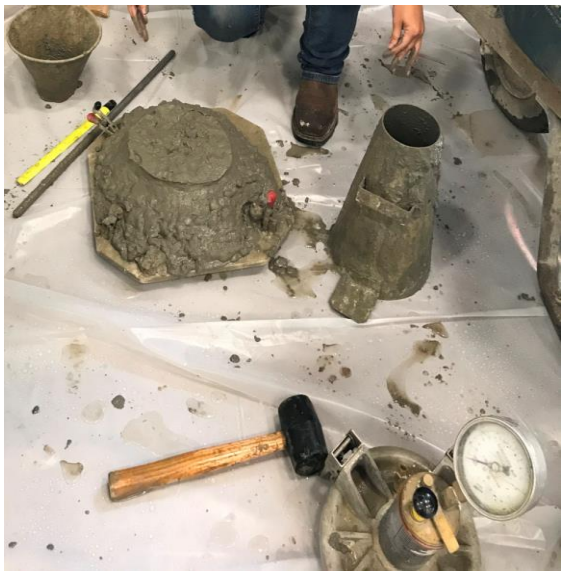

Figure 4.7 - Performing slump test on bridge deck concrete

Table 4.2: Fresh Concrete Properties

FRESH CONCRETE PROPERTIES				
	Truck 1		Truck 2	
SLUMP	9.5	in	8.25	in
UNIT WEIGHT	144.16	lb/ft^3	141.76	lb/ft^3
TEMPERATURE	91.5	°F	91.3	°F
AIR	8	%	9	%

4.3.5.2 Hardened Concrete Properties

Concrete compressive strengths were obtained at 1 d, 3 d, 7 d, 14 d, and 28 d in accordance with ASTM C39-18. Elastic modulus and splitting tensile strengths were measured in accordance with ASTM C469-14 and ASTM C496-17 respectively, and values were obtained at 1 d, 3 d, 7 d, and 28 d. Hardened concrete properties are presented in Tables 4.3-5.

Table 4.3: Hardened Concrete Compressive Strength

COMPRESSIVE STRENGTH, C39 (PSI)						
SAMPLE	1 day	3 day	7 day	14 day	21 day	28 day
1A	1410	3260	4040	4570	4880	4960
1B	1560	3620	4350	4810	5200	5530
TRUCK 1 AVERAGE	**1485**	**3440**	**4195**	**4690**	**5040**	**5245**
2A	2250	4090	4660	5310	5550	5800
2B	1940	3640	4270	4980	4880	5400
TRUCK 2 AVERAGE	**2095**	**3865**	**4465**	**5145**	**5215**	**5600**

Table 4.4: Hardened Concrete Elastic Modulus

ELASTIC MODULUS, C469 (KSI)				
SAMPLE	1 Day	3 Day	7 Day	28 Day
1A	574 (a)	3020	3350	3650
1B	2620	3090	3400	4030
TRUCK 1 AVERAGE	**2620**	**3055**	**3375**	**3840**
2A	2580	3600	4160	4180
2B	2230	3110	3390	3880
TRUCK 2 AVERAGE	**2405**	**3355**	**3775**	**4030**

NOTES:
(a): there is error in this value therefore it is disregarded in the truck 1 average.
(b): the "calculated" elastic modulus comes from aci eqn. 19.2.2.1.a –
ec = 33w^1.5*sqrt(f'c)

Table 4.5: Hardened Concrete Splitting Tensile Strength

TENSILE STRENGTH, C496 (PSI)				
SAMPLE	1 Day	3 Day	7 Day	28 Day
1A	128(a)	375	498	564
1B	217	446	525	518
TRUCK 1 AVERAGE	**217**	**411**	**512**	**541**
2A	318	524	667	648
2B	360	371	509	555
TRUCK 2 AVERAGE	**339**	**447**	**588**	**602**

NOTES:
(a): there is error in this value therefore it is disregarded in the truck 1 average.
(b): The "calculated" tensile strength comes from ACI Eqn. 19.2.4.3 – fct = 6.7*sqrt(f'c)

4.3.6 Thermal Testing

After 56 days of curing, temperature load testing was performed on the bridge deck. The load testing consisted of heating the bridge deck using heat lamps to a surface temperature between 110 °F to 120 °F, sustaining that temperature for 6 hrs., and then followed by a cooling period of 18 hrs. The cycle was repeated every 24 hrs. five days per week for approximately 8 weeks. The heating regimen closely resembles typical summer heating loads for bridge decks across the State of Oklahoma.

Heating was performed by an array of 250 W infrared heat lamps mounted atop the bridge deck. The orientation and location of the lamps is shown in Figures 4.8 and 4.9. As shown, a total of 54 heating lamps were used. Concrete temperature gradients throughout the depth of the slab, concrete steel strains, and deflections were monitored continuously for the 24-hr. cycle.

Figure 4.8 - Photograph of Thermal Loading Testing Frame Setup

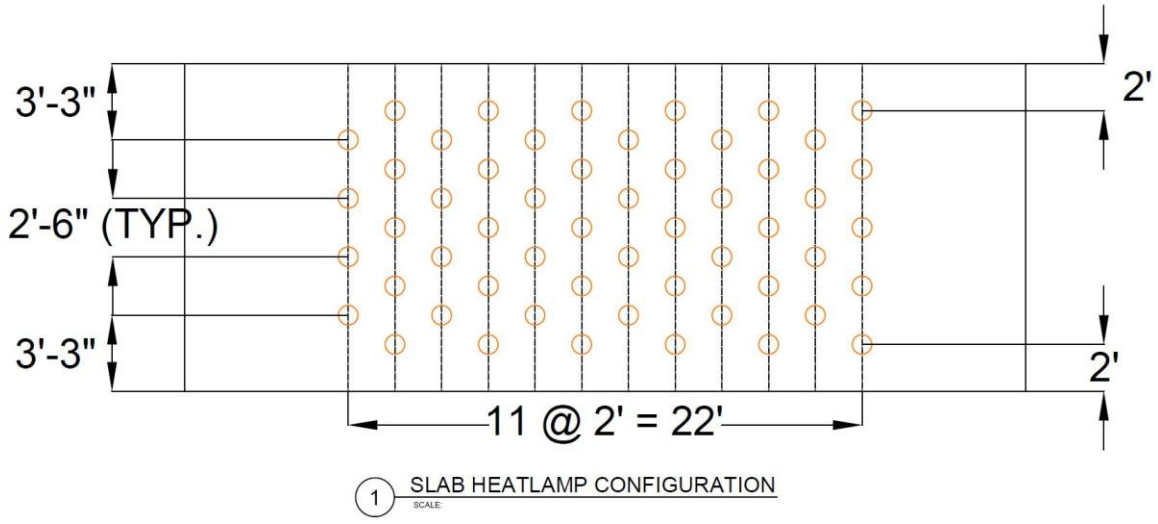

Figure 4.9 - Plan View Drawing of Thermal Loading Testing Setup: 12 rows of lamps were placed at 2 ft. c/c covering a span of 22 ft. centered on the bridge deck. Each row consisted of 4 or 5 lamps alternating amounts between rows. The total of 54 lamps were used to heat the bridge deck.

4.4 RESULTS & DISCUSSION

4.4.1 Concrete Strains

A visual representation of the strains in the concrete deck at mid-span during thermal loading for a single day is provided in Figure 4.10. A tabulation of these strains can be found in Appendix 3.

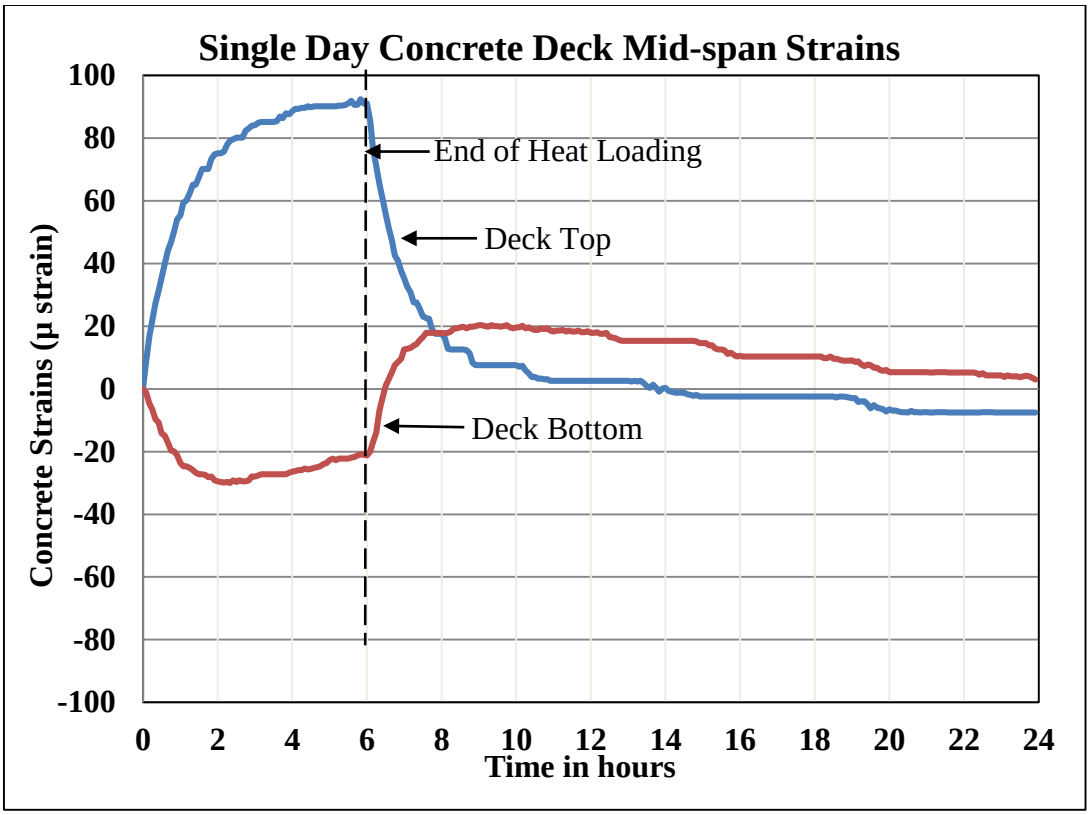

Figure 4.10 - Concrete Strains During Loading cycle on September 28, 2017: Maximum temperature values for all days of testing were recorded on this day. The maximum temperature reached 108 °F. There were slight residual strains at the end of the 24 hr. cycle. Bonded foil strain gages were placed on the top and bottom surface of the concrete slab for measurements.

From the data, we can see that as the bridge was heated the top surface of the deck experienced positive strains (lengthening) and the bottom of the deck experienced negative strains (shortening). The maximum positive strains correspond to lengthening of the concrete material caused by increases in temperature during the thermal loading. After the lamps were turned off at the 6-hr. mark of the 24-hr. cycle, the strains began merge towards zero strain. It is also observed that after the 24-hr. cycle is completed, minor residual strains remain within the concrete deck slab.

The effects of residual strains are further studied by analyzing the typical concrete strains for a 5-day loading cycle as presented in Figure 4.11.

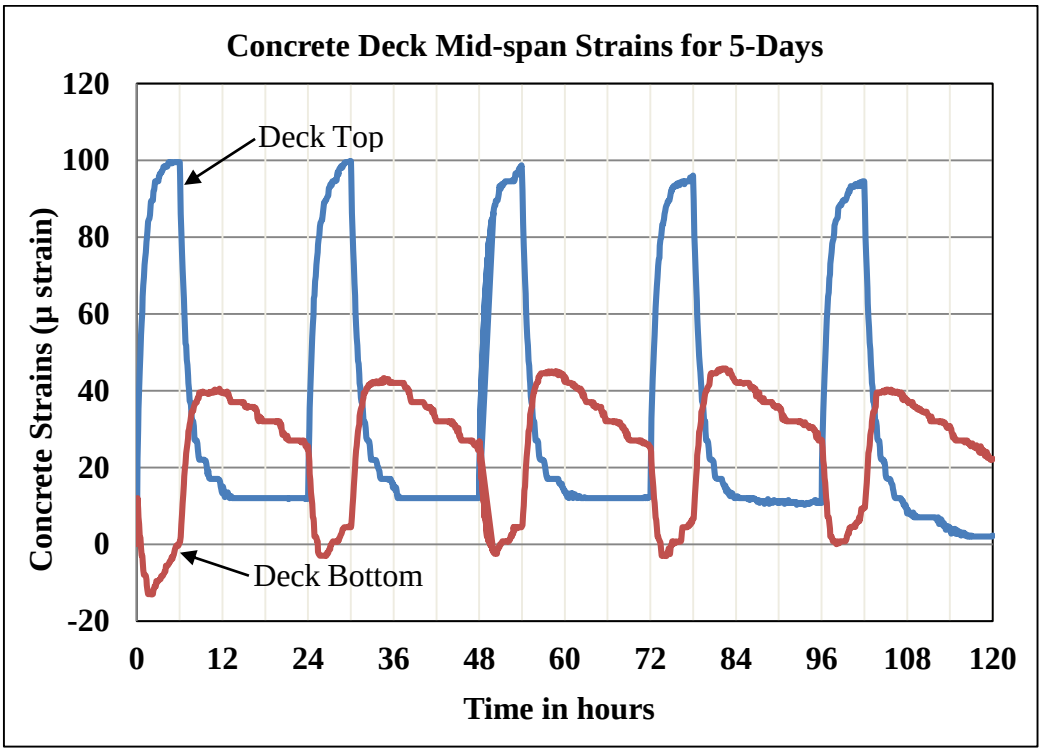

Figure 4.11 - Typical Concrete Deck Mid-Span Strains for a 5-Day Loading Cycle: The cumulative effects of residual strains throughout the week are seen by presenting the strains for a 5-day loading cycle. The strains in the top of the deck decreased over the cycle while the strains in the deck bottom increased. Bonded foil strain gages were placed on the top and bottom surfaces of the slab for measurements. The loaded cycle represented is for testing on October 2 thru October 7, 2017.

4.4.2 Steel Strains

A visual representation of the strains in the steel girders during thermal testing for a single day is provided in Figure 4.12. A tabulation of these strains can be found in Appendix 4.

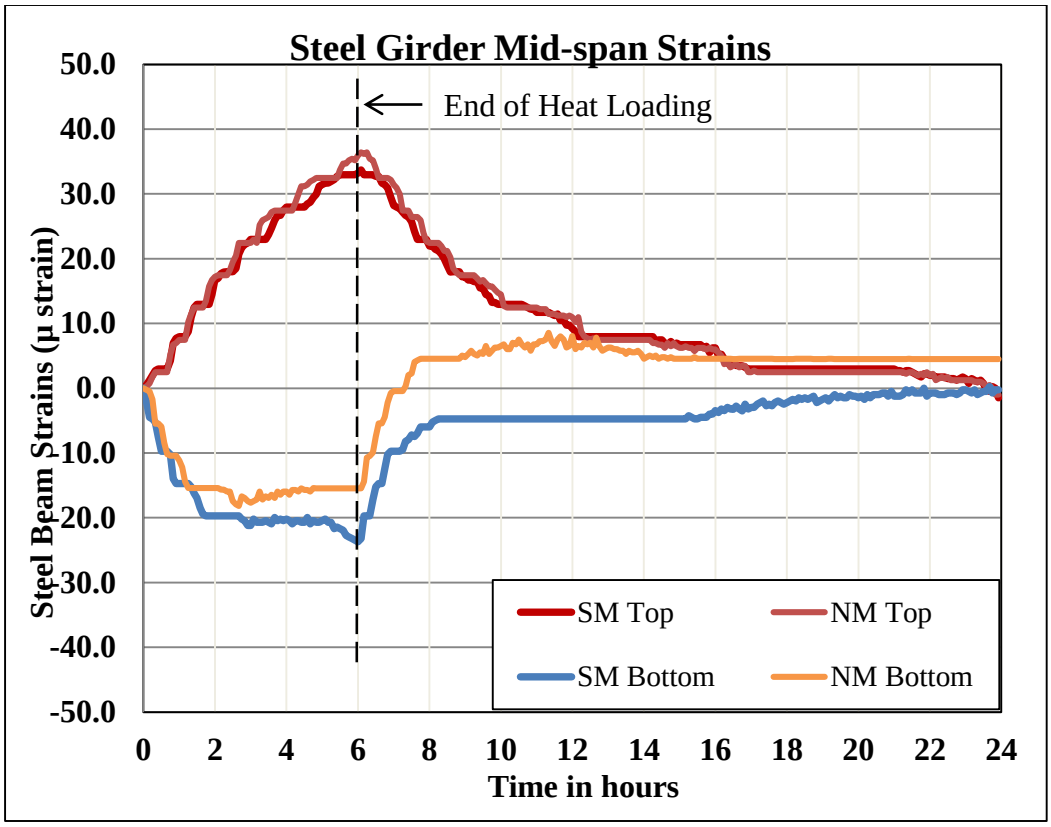

Figure 4.12 - Girder Mid-Span Strains: Steel strains during thermal loading cycle were recorded on September 28, 2017. Steel strains at the top of the girder are equal and in tension. The strains in the bottom of the girder are in compression and appear to have small unexpected differences.

During thermal loading, the top of the steel girders experienced lengthening strains. These tensile strains were approximately equal and opposite the strains experienced by the bottom surface of the concrete deck. This is to be expected as the steel girder and concrete deck are a composite system. It is also seen that the bottom of the steel girders saw compressive strains. After thermal loading, the steel girders went through the cooling phase of the 24-hr. loading cycle and the strains returned to approximately zero.

The strains in the girder at mid-span are further analyzed by observing a typical 5-day loading cycle. These strains are presented in Figure 4.13. It is observed from the figure

that there is little variation in the steel strains from cyclic loading and the strains return to approximately zero after each loading cycle.

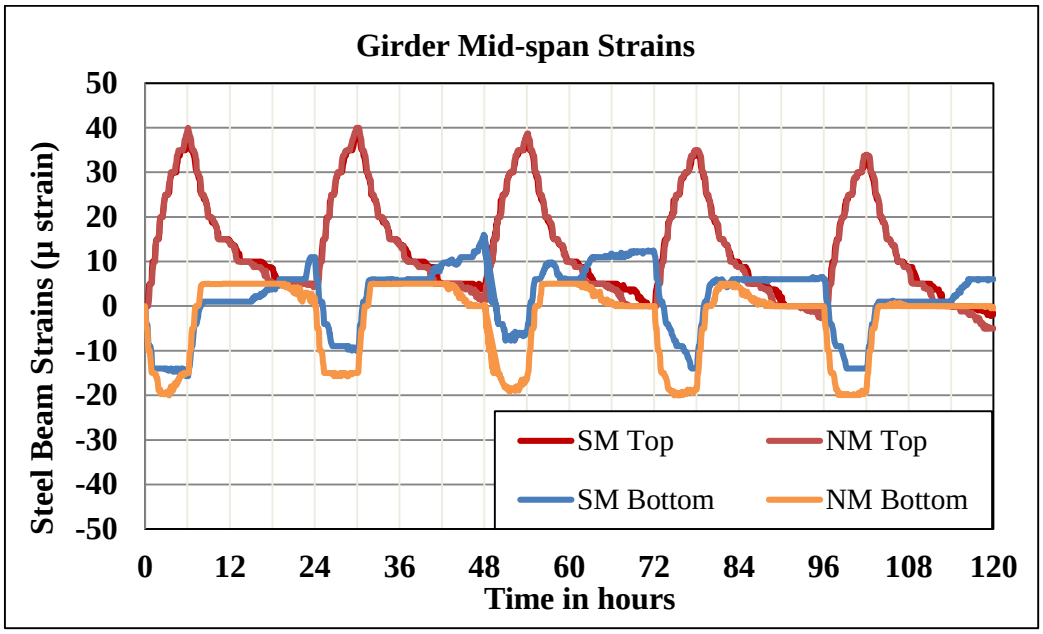

Figure 4.13 - Typical Steel Strains for a 5-Day Loading Cycle: Strains at the top of the girder are equal in tension and decrease throughout the 5-day cycle. Bottom strains have the same typical pattern with slight unexpected differences. The loaded cycle represented is for testing on October 2 thru October 7, 2017.

4.4.3 Bridge Deflections

The full-size prototype beam exhibited upward deflections of over 0.08 in. upon increasing concrete temperatures. The data and analysis indicate the deflections are caused by a combination of temperature changes and expansion of concrete. Figure 4.14 shows the deflection of the steel girders and the increase in concrete surface temperature recorded during a 24-hr. heating cycle on September 28, 2017. The various temperatures recorded over time through the depth of concrete slab at mid-span in relation to the previously shown deflections are shown in Figure 4.15.

Additionally, Figure 4.16 shows the typical deflections for a 5-day loading cycle. In the figure it is observed that there are residual deflections after a 24-hr. cycle that cause subsequent cycles to produce larger overall deflections. From these figures, it is noticed that North and South steel deflections are consistent with each other and reflects the uniform heating of the slab during testing.

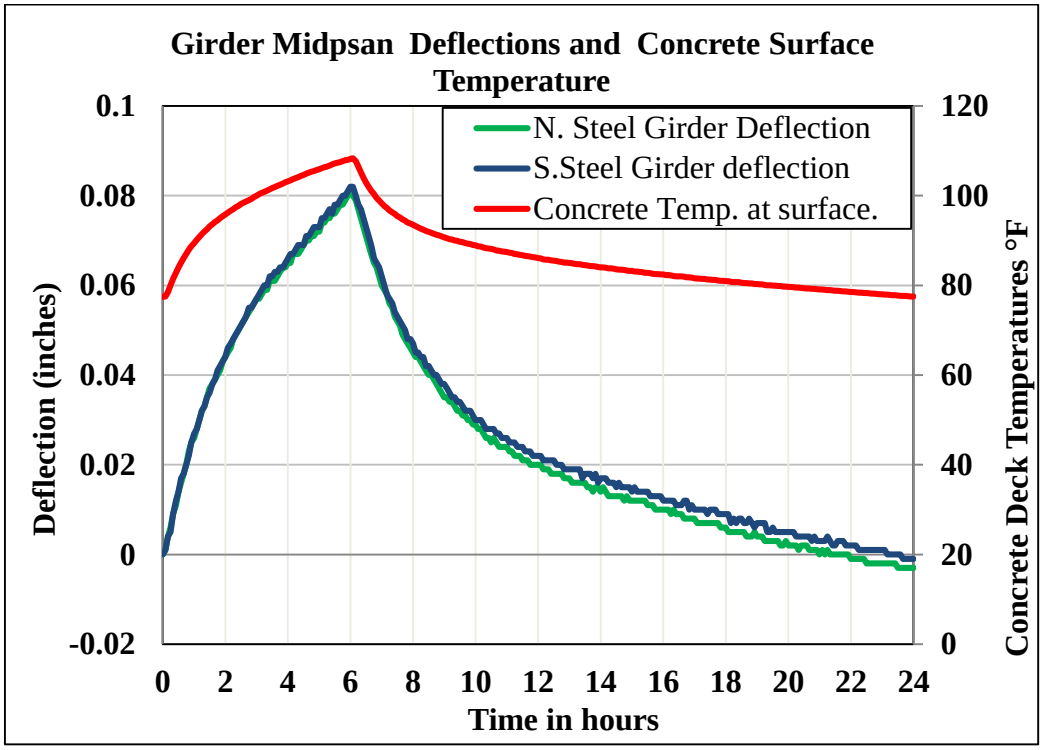

Figure 4.14 - girder mid-span deflections and concrete surface temperature on September 28, 2017: Girder deflections are consistent with the uniform heating of the concrete bridge deck. There are minimal residual deflections at the end of the 24 hr cycle.

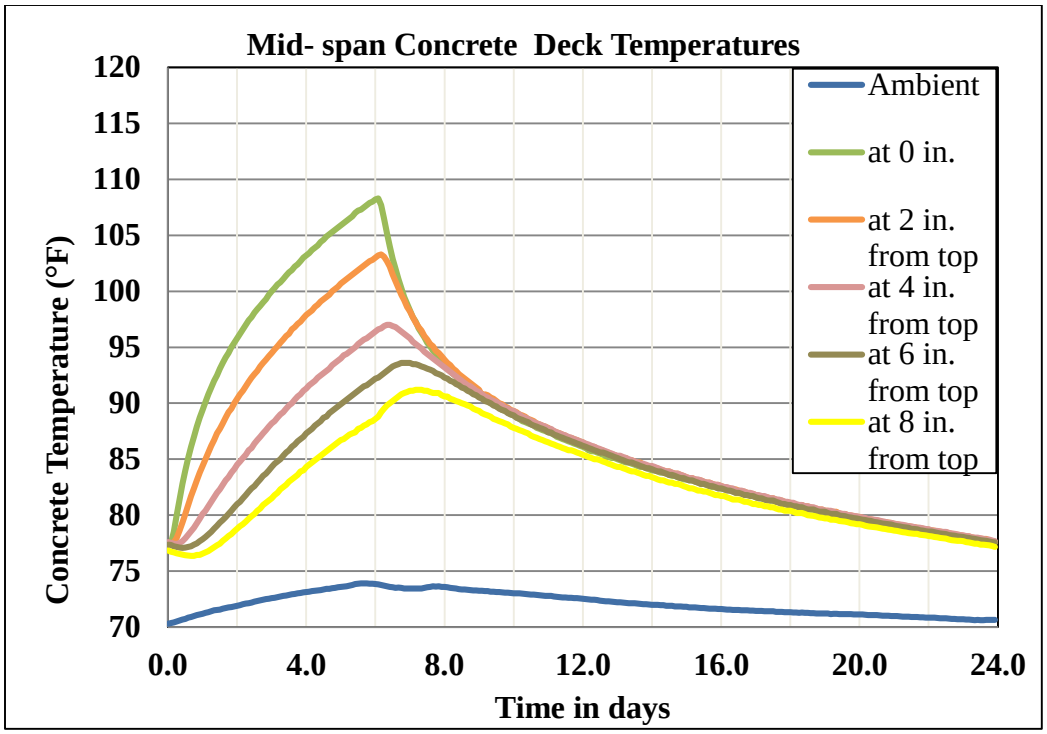

Figure 4.15 - mid-span concrete deck temperatures on September 28, 2017: Concrete temperatures are presented at depths of 0, 2, 4, 6, and 8 in. from the top of the concrete deck surface along with the ambient temperature in the lab during temperature loading. The maximum temperature at the surface it reached at the end of the 6 hr heating cycle with maximum temperatures throughout the deck being reached after the heating cycle has ended.

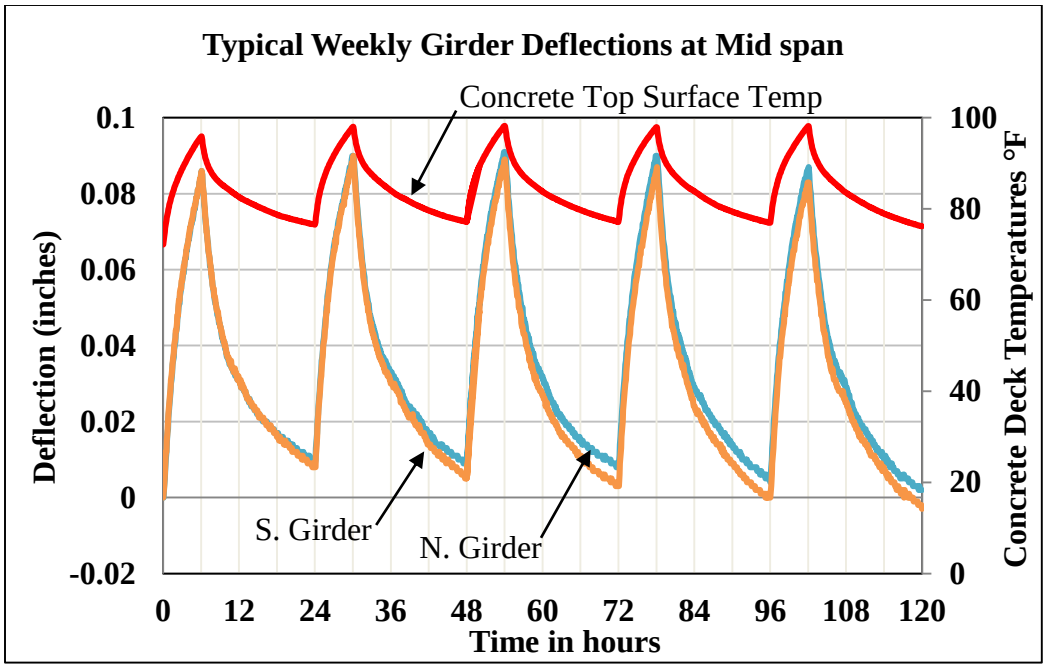

Figure 4.16 - Typical Deflections for a 5-Day Loading Cycle: There are slight residual deflections during the 5-day loading cycle resulting in slightly higher deflections throughout the week. Deflections are consistent with the heating regimen of the bridge deck. The loaded cycle represented is for testing on October 2 thru October 7, 2017.

4.4.4 Temperature Gradient

Figure 4.17 shows the maximum observed temperature gradient through the depth of the concrete slab. Values were recorded at 2-hr. time intervals during a 6 hr. testing period. Additionally, the average temperature gradient for all days of thermal load testing is presented in Figure 4.18.

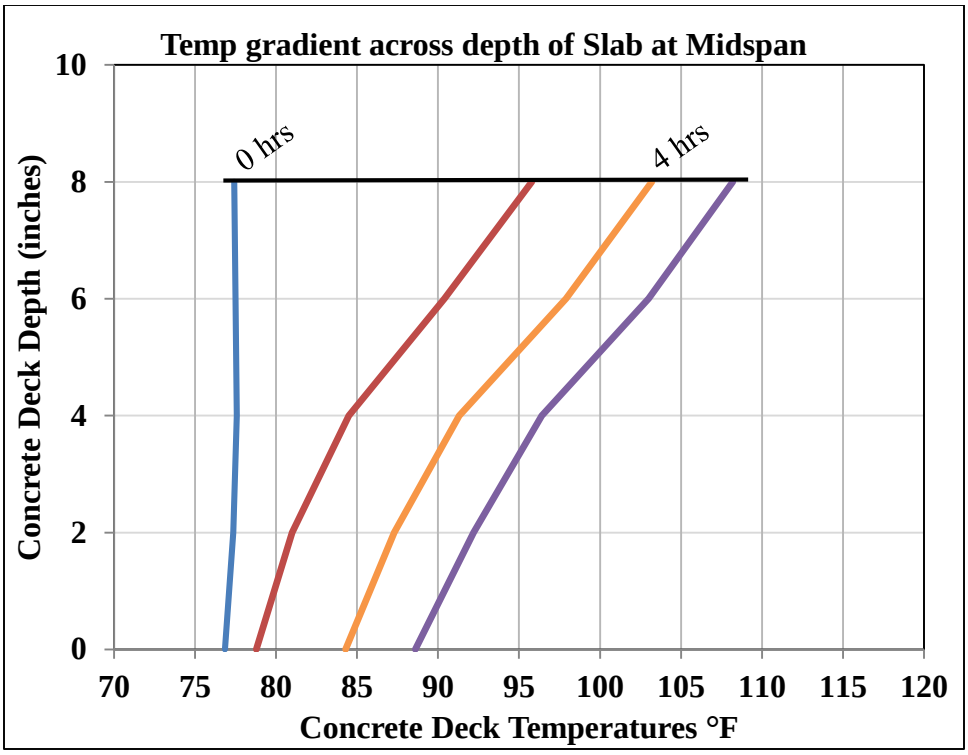

Figure 4.17 - Temperature gradient across depth of slab at mid-span for September 28, 2017: The T1 and T2 temperature values were recorded as 108 °F and 96 °F respectively after 6 hrs of heating.

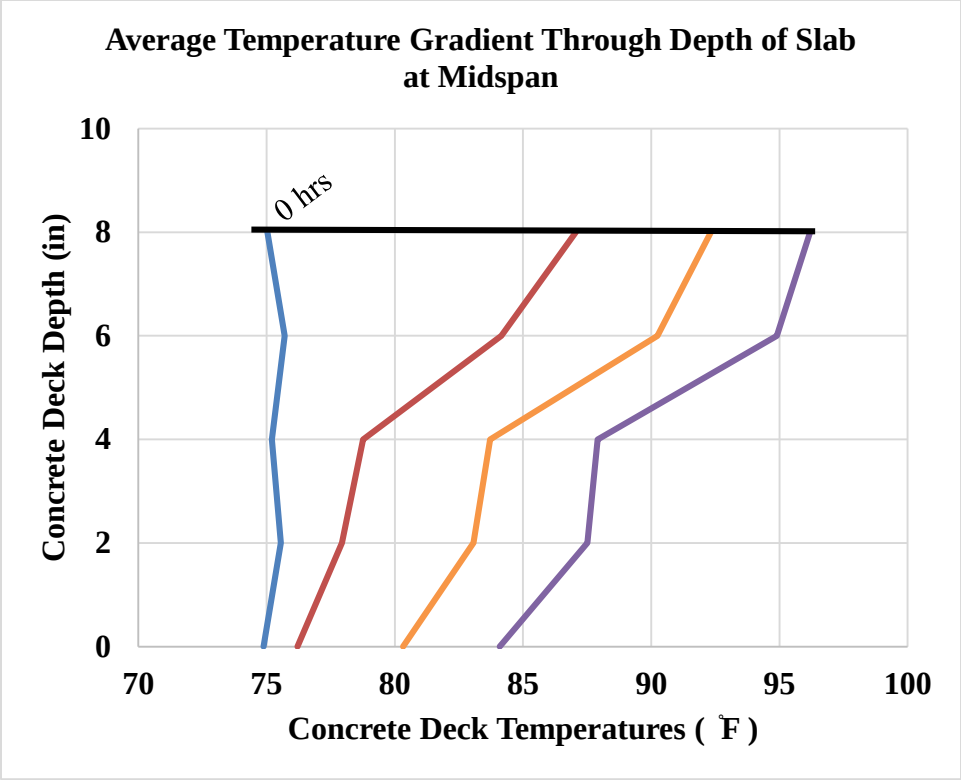

Figure 4.18 - Average Temperature Gradient for All Days of Thermal Load Testing: The average T1 and T2 values after 6 hrs of temperature loading were recorded as 96 °F and 88 °F respectively.

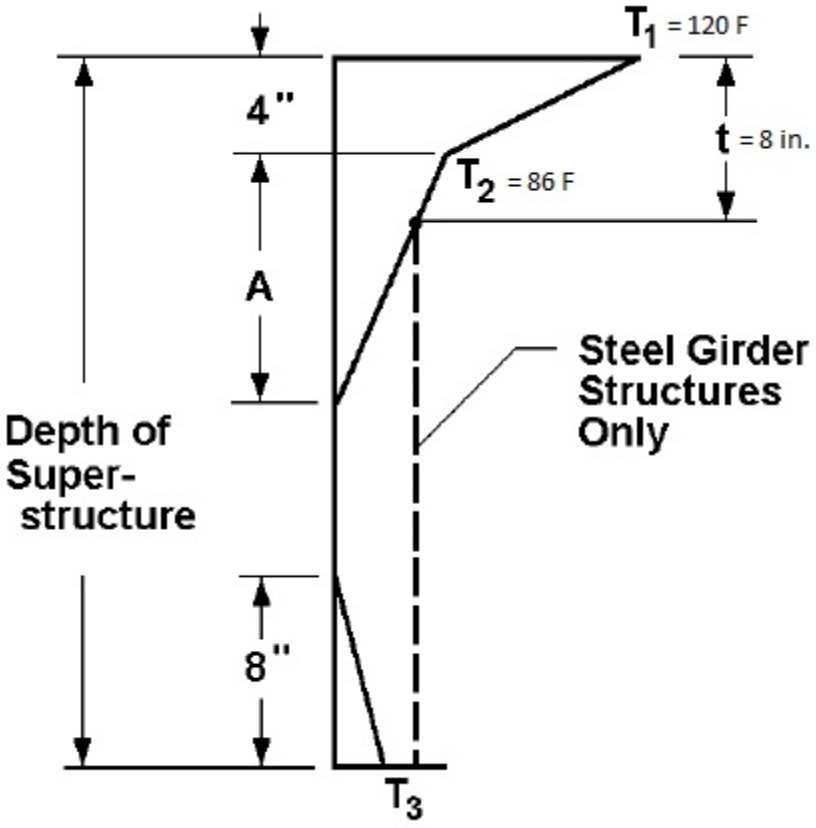

Figure 4.19 - AASHTO Specified temperature gradient: The ambient temperature at time of deck pour was 74 °F resulting in T1 and T2 values of 120 °F and 86 °F respectively (AASHTO 7th edition, Fig. 3.12.3-2)

It can be seen in Figure 4.17 that a 20 °F temperature gradient is created by the surface radiation. This temperature gradient closely resembles the AASHTO specified temperature gradient throughout the depth of the slab. The AASHTO specified temperature gradient is presented in Figure 4.19. When comparing both the maximum and average observed temperature gradients in the bridge deck to the AASHTO temperature gradient, it is evident that although the T_1 temperature of 120 °F is not reached the temperatures of approximately 96 °F and 88 °F, for the maximum and average gradients respectively, at a depth of 4 in. exceeds the AASHTO limitations of a T_2 temperature of 86 °F. AASHTO T_1 and T_2 values are determined based on region and

ambient temperature at time of deck casting. For this bridge deck, 46 °F and 12 °F were added to the ambient temperature of 74 °F to obtain temperature gradient values for T_1 and T_2 respectively. Underestimating the effects of the temperature gradient can significantly affect tensile cracks and stress distributions in the bridge deck.

4.5 Conclusion

From analysis of the data, the following conclusions can be obtained:

- Radiant heat loads produced upward deflections in composite bridges.
- The upward deflection with 108 °F measured just below the concrete surface was about 0.08 in. for the 38.83 ft span.
- The measured temperature gradient through the depth of the slab was as high as 20 °F after 6 hrs. of radiant heat exposure.
- It is suggested that additional research be performed on various bridge types to determine the accuracy of the AASHTO temperature gradient in other cases.
- Additional research and analysis is needed for actual highway bridges.

CHAPTER V

CONCLUSION

5.1 SUMMARY

The initial deflections in the steel girders due to the self-weight of the concrete were approximately 0.40 in. Additionally, the concrete deck overhang deflected about 0.85 in. downward indicating that a major component of excessive deflections in bridge decks is poor bracing during construction. During hydration, the concrete reached a maximum temperature of nearly 110 °F and experienced upward deflections of 0.1 in. 12 hrs. after slab cast. The bridge deck then began to cool and downward deflections gradually increased. After 28 days, the steel beams and concrete deck both deflected an additional 0.19 in. downward for total deflections approximately 0.6 in. and 1.1 in. respectively.

The strains during this time were also used to determine the movement of the neutral axis through the section and the time after cast in which composite action occurred. It was found that after 72 hrs., the neutral axis reached a height of approximately 24.4 in. The time of fully composite action was found to occur around 6 hrs. after slab cast.

During thermal load testing on the full sized prototype bridge it was found that thermal induced strains and deformations in composite bridges and bridge decks are significant. Normal temperature ranges for summertime deck heating with a maximum surface

temperature of approximately 120 °F caused upward deflections of more than 0.08 in. when an area of 22 ft x 14 ft was subjected to the thermal loading. If the full span of 40 ft were subjected to the same thermal loading, it is calculated that upward deflections would be in excess of 0.14 in. The prototype bridge measurements show the significance of temperature gradients produced by summertime heat loadings and should be investigated further.

5.2 CONCLUSIONS

The following conclusions have been drawn from Chapter 3:

- Measured deflections caused by the self-weight of the concrete was 0.38 in. and 0.40 in. on the two girders. This nearly matches the deflections computed using beam theory, a span of 38.83 ft. and a unit weight of concrete of 150 pcf, which yielded a calculated deflection of…
- Deflections in the concrete overhang were 0.45 in. more than the deflection of the girders.
- Further research is needed to design a more adequate bracing system to reduce initial deflections.
- Further research should be performed to determine the influence of creep on early age deflections.
- The bridge deflected upward approximately 0.08 in. due to the heat of hydration of the concrete deck, which also proves composite action.
- The bridge deflected downward as the deck cooled.

- Shrinkage of the concrete deck increased after the wet curing was removed at 14 days. Also, the bridge's downward deflection accelerated after the wet curing was removed indicating a correlation between slab shrinkage and downward deflection of the bridge.

Conclusions from Chapter 4:

- Radiant heat loads produced upward deflections in composite bridges.
- The upward deflection with 108 °F measured just below the concrete surface was about 0.08 in. for the 38.83 ft span.
- The measured temperature gradient through the depth of the slab was as high as 20 °F after 6 hrs. of radiant heat exposure.
- It is suggested that additional research be performed on various bridge types to determine the accuracy of the AASHTO temperature gradient in other cases.
- Additional research and analysis is needed for actual highway bridges.

REFERENCES

AASHTO LRFD bridge design specifications

Abdelmeguid, I. S. (2016). Shrinkage Induced Deformations in Composite Steel and Concrete Bridges. B. W. Russell, T. M. Ley and J. Hartell.

Alexander, S. (2003). "Concrete shrinkage affects composite steel beams." New steel construction **11**(3): 22-23.

Azizinamini, A. and A. Yakel (2006). "Delayed development of composite action in steel girder bridges." Bridge Structures: Assessment, Design and Construction **2**(3): 119-132.

El-Tayeb, E. H., S. E. El-Metwally, H. S. Askar and A. M. Yousef (2017). "Thermal analysis of reinforced concrete beams and frames." HBRC Journal **13**(1): 8-24.

Fu, H. C., S. F. Ng and M. S. Cheung (1990). "Thermal behavior of composite bridges." Journal of Structural Engineering (United States) **116**(12): 3302-3323.

Hadidi, R., M. A. Saadeghvaziri and C. T. T. Hsu (2003). "Practical tool to accurately estimate tensile stresses in concrete bridge decks to control transverse cracking." Practice Periodical on Structural Design and Construction **8**(2): 74-82.

Imbsen, R. A., D. E. Vandershaf, R. A. Schamber and R. V. Nutt (1985). "THERMAL EFFECTS IN CONCRETE BRIDGE SUPERSTRUCTURES." National Cooperative Highway Research Program Report.

Khan, I., A. Murray, A. Castel and R. I. Gilbert (2015). Experimental and Analytical Study of Creep and Shrinkage in Early-Age Concrete. 10th International Conference on Mechanics and Physics of Creep, Shrinkage, and Durability of Concrete and Concrete Structures. C. Hellmich, B. Pichler and J. Kollegger. Reston, VA, Reston, VA: American Society of Civil Engineers**:** 1066-1075.

Krkoska, L. and M. Moravcik (2017). Monitoring of temperature gradient development of highway concrete bridge. **117:** <xocs:firstpage xmlns:xocs=""/>.

Kwon, G., B. Hungerford, H. Kayir, B. Schaap, Y. K. Ju, R. Klingner and M. D. Engelhardt (2007). Strengthening existing non-composite steel bridge girders using post-installed shear connectors.

Ley, T. (2012). Portland Cement Hydration.

ODOT. (2018). "Deficient Bridges: Replacement and Rehabilitation Progress." from https://ok.gov/odot/Bridges.html.

Oehlers, D. J. and M. A. Bradford (2013). Composite Steel and Concrete Structures: Fundamental Behaviour: Fundamental Behaviour, Elsevier.

Olsson, D., R. Hällmark and P. Collin (2017). Achieving Composite Action in Existing Bridges: With post-installed shear connectors.

Reynolds, J. C. (1972). Thermal Stresses and Movements in Bridges Masters Theses, Missouri University of Science and Technology.

Rodriguez, L. E., P. J. Barr and M. W. Halling (2014). "Temperature effects on a box-girder integral-abutment bridge." Journal of Performance of Constructed Facilities **28**(3): 583-591.

Rojas, E. (2014). Uniform temperature predictions and temperature gradient effects on I-girder and box girder concrete bridges. P. J. Barr, J. Bay and M. Halling, ProQuest Dissertations Publishing.

Subramaniam, K., J. Kunin, R. Curtis and D. Streeter (2010). "Influence of Early Temperature Rise on Movements and Stress Development in Concrete Decks." Journal of Bridge Engineering(1): 108-116.

Taly, N. (2014). Highway bridge superstructure engineering: LRFD approaches to design and analysis, CRC Press.

APPENDICES

APPENDIX 1 – AGGREGATE PROPERTIES

Appendix 1.1 – Coarse Aggregate Properties

Table A.1.1.1 – Sieve Analysis of Quapaw Rock

Sieve	Weight Retained (g)	% Retained	% Passing
1 1/2"	0	0	100
1"	1	2	98
3/4"	8	35	62
1/2"	12	50	12
3/8"	2	10	2
No. 4	0	2	0
No. 8	0.0	0.0	0.2
Pan	0.0	0.2	0.0
Total	23.53	100.00	

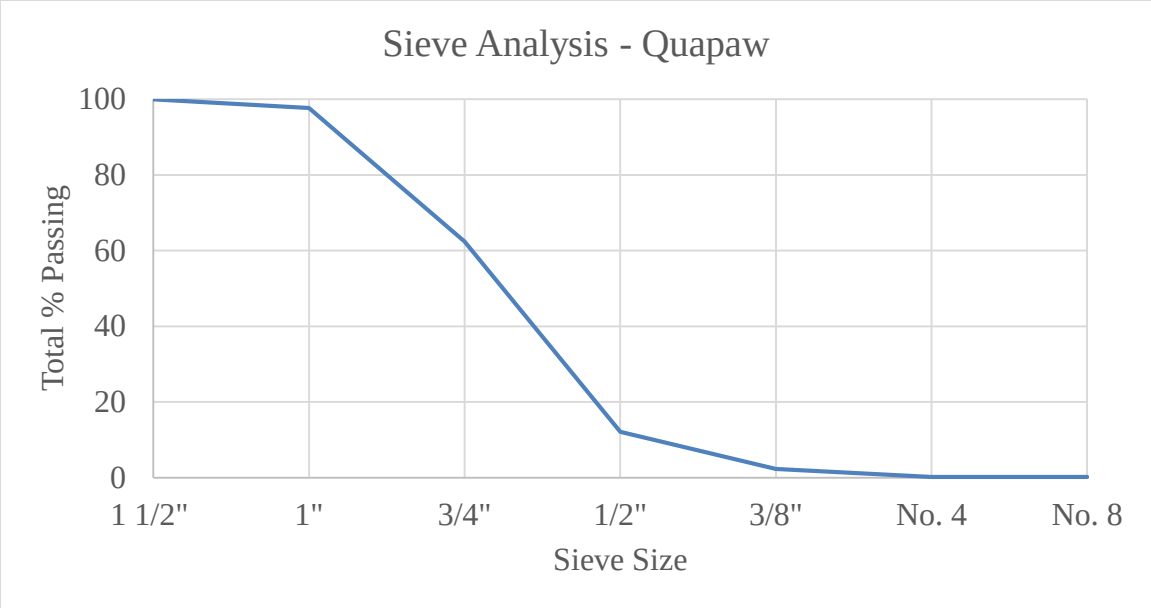

Figure A.1.1.1 – Sieve Analysis Results of Quapaw Rock

Table A.1.1.2 – Physical Properties of Quapaw Rock

Quapaw Properties	
Specific Gravity	2.86
Absorption	1.13%
DRUW	100.69 lb/ft^3

Appendix 1.2 – Fine Aggregate Properties

Table A.1.2.1 – Sieve Analysis of Guthrie Sand

Seive	Weight Retained (g)	% Retained	% Passing
No. 4	1.6	0	100
No. 8	16.5	4	96
No. 16	69.4	17	83
No. 30	168	51	49
No. 50	186.2	88	12
No. 100	56	99	1
No. 200	4	100	0.1
Pan	0.6	100	0.0
Total	502.3		

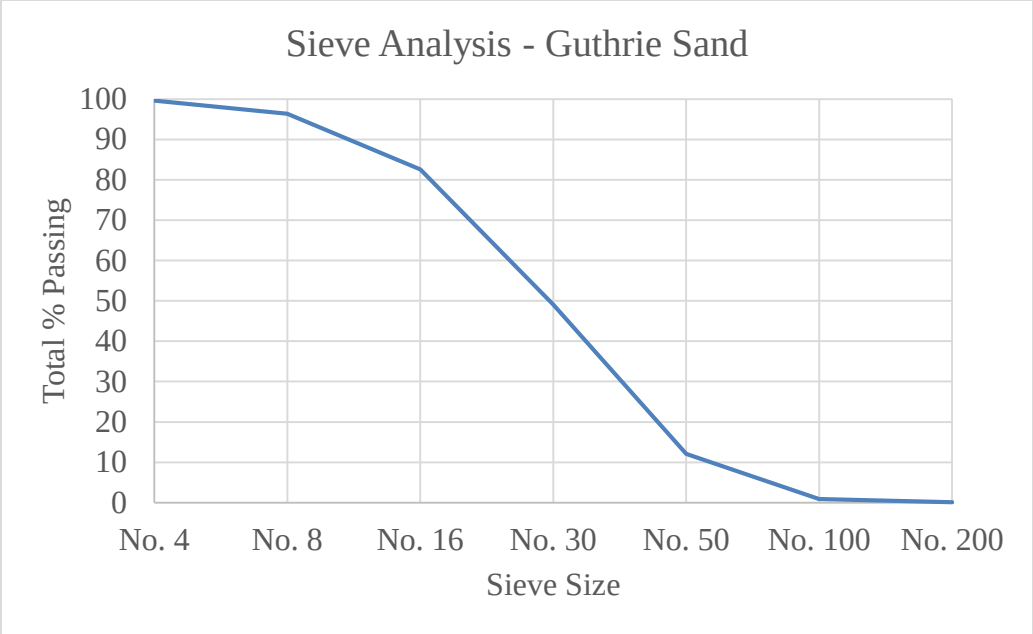

Figure A.1.2.1 – Sieve Analysis Results of Guthrie Sand

Table A.1.2.2 - Physical Properties of Guthrie Sand

Guthrie Sand Properties	
Specific Gravity	2.63
Absorption	0.46%
Fineness Modulus	2.59

APPENDIX 2 – CONCRETE STRAINS AT MID-SPAN DURING THERMAL LOADING

Table A.2.1 – Concrete Strains at Mid-Span on September 28, 2017. Strain are measured using bonded foil strain gages on the top and bottom surfaces of the concrete deck.

TIME	TOP STRAIN	BOTTOM STRAIN
(hr)	($x10^{-6}$ in/in)	
0	0	0
1	55	-24
2	75	-29
3	84	-28
4	89	-26
5	90	-23
6	91	-21
7	35	13
8	18	18
9	8	20
10	8	20
11	3	18
12	3	18
13	3	15
14	0	15
15	-2	15
16	-2	11
17	-2	10
18	-2	10
19	-3	9
20	-6	5
21	-7	5
22	-8	5
23	-7	4
24	-7	3

APPENDIX 3 – GIRDER STRAINS AT MID-SPAN DURING THERMAL LOADING

Table A.3.1 – Girder Strains at Mid-Span on September 28, 2017. Strain are measured using bonded foil strain gages on the North on South Girders with distances of 4 in. from the top and bottom surfaces of the girder.

	SOUTH GIRDER		NORTH GIRDER	
TIME	Top	Bottom	Top	Bottom
0	0	0	0	0
1	8	-15	8	-11
2	17	-20	17	-15
3	23	-21	23	-18
4	28	-20	27	-16
5	31	-21	32	-15
6	33	-24	36	-15
7	28	-10	31	-1
8	22	-6	23	5
9	17	-5	18	5
10	13	-5	15	7
11	12	-5	13	7
12	9	-5	11	8
13	8	-5	8	6
14	8	-5	8	5
15	7	-5	6	5
16	6	-4	6	5
17	3	-3	3	5
18	3	-2	3	5
19	3	-2	3	5
20	3	-2	3	5
21	3	-1	3	5
22	2	-1	2	5
23	2	0	1	5
24	-2	0	-1	5

VITA

Alanna Webb

Candidate for the Degree of

Master of Science

Thesis: BEHAVIOR OF COMPOSITE BRIDGES AT EARLY AGES AND UNDER THERMAL LOADING

Major Field: Civil Engineering

Biographical:

Education:

Completed the requirements for the Master of Science in Civil Engineering at Oklahoma State University, Stillwater, Oklahoma in December, 2018.

Completed the requirements for the Bachelor of Science in Civil Engineering at Oklahoma State University, Stillwater, Oklahoma in May, 2016.